Since January 2020 Elsevier has created a COVID-19 resource centre with free information in English and Mandarin on the novel coronavirus COVID-19. The COVID-19 resource centre is hosted on Elsevier Connect, the company's public news and information website.

Omega 119 (2023) 102872

Contents lists available at ScienceDirect

Omega

journal homepage: www.elsevier.com/locate/omega

A robust optimization problem for drone-based equitable pandemic vaccine distribution with uncertain supply☆

Xin Wang[a,b], Ruiwei Jiang[c], Mingyao Qi[b,*]

[a] Department of Industrial Engineering, Tsinghua University, Beijing 100084, China
[b] Logistics and Transportation Division, Shenzhen International Graduate School, Tsinghua University, Shenzhen 518055, China
[c] Department of Industrial and Operations Engineering, University of Michigan, Ann Arbor, MI 48103, USA

ARTICLE INFO

Article history:
Received 8 January 2023
Accepted 15 March 2023
Available online 21 March 2023

Keywords:
Pandemic vaccine distribution
Drone delivery
Robust optimization
Uncertain supply
Facility location

ABSTRACT

Widespread vaccination is the only way to overcome the COVID-19 global crisis. However, given the vaccine scarcity during the early outbreak of the pandemic, ensuring efficient and equitable distribution of vaccines, particularly in rural areas, has become a significant challenge. To this end, this study develops a two-stage robust vaccine distribution model that addresses the supply uncertainty incurred by vaccine shortages. The model aims to optimize the social and economic benefits by jointly deciding vaccination facility location, transportation capacity, and reservation plan in the first stage, and rescheduling vaccinations in the second stage after the confirmation of uncertainty. To hedge vaccine storage and transportation difficulties in remote areas, we consider using drones to deliver vaccines in appropriate and small quantities to vaccination points. Two tailored column-and-constraint generation algorithms are proposed to exactly solve the robust model, in which the subproblems are solved via the vertex traversal and the dual methods, respectively. The superiority of the dual method is further verified. Finally, we use real-world data to demonstrate the necessity to account for uncertain supply and equitable distribution, and analyze the impacts of several key parameters. Some managerial insights are also produced for decision-makers.

1. Introduction

The outbreak of coronavirus disease 2019 (COVID-19) has caused severe negative impacts on both social life and the economy across the globe. More than 666 million confirmed cases and 6 million deaths have been reported by the end of 2022, according to worldometers.info. The cumulative loss of global GDP over 2020 and 2021 due to the COVID-19 crisis was estimated to be around 9 trillion dollars, according to the International Monetary Fund (IMF). Although government measures related to lockdowns and social distancing can effectively prevent the spread of the pandemic, the only way to eradicate coronavirus is through widespread vaccination [30]. Within one year of the first confirmed case, over a hundred types of COVID-19 vaccines are in development, eleven of which are in phase III trials [59]. After the effective vaccines are licensed and become available, how to efficiently distribute vaccines worldwide and inoculate all populations is absolutely essential [54].

The vaccine distribution chain can be categorized into four consecutive stages: sourcing, storage, transportation, and administration [19]. The last decade has witnessed many studies on each stage. For the sourcing stage, studies are mainly on where, when, how many and at what price to acquire the needed vaccines (e.g., Pazirandeh [49]). In the storage stage, a vital consideration is how to make vaccines thermostable while minimizing the cost (e.g., Lee et al. [38]), or managing inventory to rule out expiry wastage. Transportation is to deliver vaccines from providers to the users, typically through a hierarchical transportation network. For example, vaccines may go through national, regional, district, and local health facilities before applying to people [36]. Finally, administration is to schedule and perform the vaccination, for example, in a health facility. As emerging transportation technologies like drones are practically applied to vaccine delivery, the operation mode of the vaccine distribution chain produces new changes. Meanwhile, the sudden outbreak of the pandemic brings more challenges to the administration of vaccines as the supply encounters a shortage. These backgrounds motivate our study on the joint transportation and administration problem, and we further justify it in the following part of this section.

☆ Area: Production Management, Scheduling and Logistics. This manuscript was processed by Associate Editor Otto.

* Corresponding author.
E-mail addresses: wangxin16@mails.tsinghua.edu.cn (X. Wang), ruiwei@umich.edu (R. Jiang), qimy@sz.tsinghua.edu.cn (M. Qi).

https://doi.org/10.1016/j.omega.2023.102872
0305-0483/

Drone delivery has become an ideal option for vaccine distribution in recent years [28]. Unlike common products, vaccines are temperature sensitive and must be continuously preserved in the proper condition through a cold supply chain. Otherwise, the potency could be diminished or even destroyed [58]. Due to the limited shelf life of vaccines, delivery time is also critical. Unfortunately, the lack of qualified infrastructures (e.g., electric power, refrigerator equipment), poor road conditions, and inadequate trained personnel pose a significant challenge to vaccine distribution in rural areas [12]. According to their high speed, reduced traffic restrictions, and low manpower need, many governments have attempted to utilize the emerging technologies of drone delivery to get out of the predicament. In February 2021, Zipline made the first attempt to deliver COVID-19 vaccines to rural areas in Ghana via drones. It took only 30 to 40 min to complete each delivery, while the traditional transportation could hardly reach the place [57]. The application of drones allows for more frequent deliveries, less inventory, and less need for cold chain equipment. Thus, our research digs into the drone-based vaccine distribution problem, where drones are employed to deliver vaccines rapidly to health facilities in vulnerable places. Although there are lots of studies focusing on drone delivery optimization problems (see, e.g., Chung et al. [15], Macrina et al. [43], Otto et al. [48]), very few of them concern vaccine distribution.

Generally, a vaccine distribution chain is subject to both supply and demand uncertainty [41]. However, in the early stages of vaccine distribution after the pandemic outbreak, the supply of vaccines is pretty scarce, then demand is supposed to outstrip supply. Due to the limited production and unstable transportation, the number of vaccines arriving at a distribution center in each time period is random, and it is difficult to obtain the accurate value. That means the corresponding demand can be scheduled as long as there is an allocated supply. Hence, the uncertainty in supply becomes the dominant barrier to effective vaccination regarding vaccine shortages. Neglecting the impact of this uncertainty, the decision can be unsatisfactory in real-life contexts, such as incurring unmet vaccination appointments or wasted vaccines if the arrived vaccines are less or more than the pre-assigned volume, respectively. Nonetheless, even the research addressing any uncertain characteristic is rather limited in the vaccine distribution problem [19]. To our best knowledge, little attention has been paid to supply uncertainty in this field. Generally, stochastic programming (SP) and robust optimization (RO) are the most common methods for solving uncertain problems with random parameters. Unlike SP requiring accurate probability information, RO uses an uncertainty set without the probability distribution to characterize the uncertain attributes and focuses on the worst-case optimization. In practice, it is often difficult to obtain sufficient information to support a probability distribution of uncertain parameters [2,9,14,47,52]. Hence, this research adopts an RO method to hedge the influence of supply uncertainty on vaccine transportation and administration.

Equity is another critical issue that needs to be considered for vaccine distribution. It is particularly essential for not only justice but also extinguishing the overall severity of the pandemic [1,37]. If vaccines are distributed inequitably, a large number of people will be exposed to the virus, leading to the potential for high transmission rates and fertile ground for the development and spread of new variants [56]. However, according to the data from WHO, UNDP, Oxford University [60], as of Nov 2021, only 7.46% of people in low-income countries have received at least one dose of COVID-19 vaccine, while the proportion in high-income countries is 63.87%. Besides, the gap in the coverage rate between urban and rural areas within a region is also considerable. In this regard, we propose several equity-related constraints to develop a practical approach for equitable distribution.

Most types of COVID-19 vaccines (e.g., Pfizer-BioNTech, Moderna, Sinovac Biotech) require multiple doses for high efficacy. The first two doses are especially significant during the early stages and should be administered only three to four weeks apart [55]. The consideration of the two-dose regimen is important when scheduling vaccinations [8]. In summary, this research studies a drone-based two-dose vaccine distribution problem with uncertain supply by addressing the following three questions:

1. How many health facilities should be selected for vaccination, and where are they located to balance the social and economic benefits?
2. How to equitably schedule vaccinations or assign vaccines to the selected health facilities and then to the demand sites for each period?
3. How many drones should be deployed for vaccine transportation?

The main contributions of this paper lie in the following aspects:

1. We address the supply rather than demand uncertainty in the vaccine distribution problem with a robust optimization method, which could better fit the vaccine shortage situation during the early pandemic outbreaks;
2. This is the first study considering a joint vaccination facility location, transportation capacity design, and vaccination scheduling problem, which is tailored to addressing vaccination difficulties in rural or remote areas using drone delivery technologies;
3. We adopt a two-stage RO framework with a budgeted uncertainty set to deal with the uncertain problem, and propose two tailored column-and-constraint generation (C&CG) algorithms to solve the model exactly. The subproblems of C&CG are solved via the vertex traversal and the dual methods, respectively. In particular, a mixed-integer linear programming (MILP) formulation is provided for the nonlinear dual subproblem;
4. We use real-world data to justify the model and demonstrate the necessity of considering equity and uncertain supply, which leads to several managerial insights for decision-makers.

The rest of this paper is organized as follows. Section 2 gives a brief review of the related literature. Section 3 elaborates the problem and proposes a two-stage robust formulation. Section 4 provides the two solution methods based on the C&CG algorithm. Section 5 uses the case study to demonstrate the efficiency of the algorithm and analyze the problem. Finally, in Section 6, we conclude this study and give directions for future research.

2. Literature review

A systematic review of the literature on the vaccine supply chain is presented in Duijzer et al. [21] and Lopes et al. [42]. Another study by De Boeck et al. [19] summarizes the papers on the scope of vaccine distribution and categorizes them based on their decision levels into strategic, tactical, and operational problems. In this section, we first review the related studies according to the decision level and then analyze the research addressing specific characteristics of pandemic vaccination, i.e., the equity consideration and the uncertain nature. We also examine a more general location-transportation problem (LTP), which we believe is relevant to our study.

2.1. Vaccine distribution problems

Strategic level studies The problems involving a strategic level receive the most research attention, where long-term decisions such

as facility location and allocation, and vial size design are addressed. Lim et al. [40] developed four types of coverage models to determine the location of outreach vaccination facilities. It is also common to extend the strategic problem to two levels, incorporating tactical decisions. Li et al. [39] provided a mixed-integer nonlinear programming model for a location problem, incorporating the assignment of medical staff and their work schedules, which resolves conflicting objectives involving the travel distance, number of opened facilities, and operational cost. Generally, vaccination may last for multiple periods, during which parameters such as demand, supply, and cost may change over time. A multi-period strategy addressing time-dependent parameters seems more appropriate. In this regard, Azadi et al. [5] maximized the vaccination coverage rate by deciding the tier of the supply chain and scheduling the transportation and inventory replenishment in each period. Chen et al. [11] investigated a location-allocation and inventory problem in developing countries to improve the number of fully immunized children. Rastegar et al. [51] proposed an MILP model for a location-inventory problem of influenza vaccines during the COVID-19 pandemic, in which the assumptions on multi-group allocation, vaccine shortage, budget constraints, and time-dependent capacities are included. Tavana et al. [54] later extended the problem to a multi-product model with three types of COVID-19 vaccines, requiring cold, very cold, and ultra-cold refrigeration, respectively. Lai et al. [35] studied an integrated planning problem that jointly optimizes the vaccination locations, the planning for health staff, vaccine ordering, and inventory in each period. Demand uncertainty is addressed via a two-stage stochastic programming method.

Tactical level studies Tactical decisions are made with mid-term impacts, such as inventory, vaccine flow (e.g., vaccine transportation, plan, assignment), and service capacities (e.g., storage, transportation, and staff capacity). Balcik et al. [7] investigated an equitable vaccine allocation problem within the country in terms of vaccine shortages, and proposed a new objective that minimizes the total deviation from the equitable coverage levels. Jahani et al. [31] sought to efficiently and effectively distribute and store the COVID-19 vaccines, considering the congestion in the vaccination procedure. They conducted a multi-period queuing-based model to minimize the total cost and the expected waiting time. Georgiadis and Georgiadis [25] investigated the COVID-19 vaccine distribution chain from both tactical and operational levels, optimizing the vaccine transportation, inventory, staff assignment, and daily scheduling of vaccination. The wastage of the vaccine is explicitly considered, and a rolling-horizon algorithm is conducted to cope with the demand fluctuations. Additional distribution problems for COVID-19 vaccines involving tactical decisions can also be found in Kumar et al. [34], Rahman et al. [50].

Operational level studies For research at this level, short-term decisions are captured, such as administration and daily scheduling. Azadi et al. [6] explored a vaccination problem considering open vial wastage, which optimizes the vaccine ordering and vial opening decisions for various vial-size vaccines. Mofrad et al. [46] modeled the vaccine administration problem as a Markov decision process (MDP), which dynamically determines the open hours of a clinic, the current vial inventory, and the remaining open days, and seeks to maximize the administrations of vaccines. Fadaki et al. [23] analyzed a vaccine allocation and administration problem via a case study of Australia incorporating the risk of the uninoculated population, while Jarumaneeroj et al. [32] studied a case of Thailand addressing the pandemic transmission. Zhang et al. [65] developed a vaccination scheduling model which determines the location and service sequence of vaccination sites, as well as the assignment, acceptance, and rejection of each appointment. In addition to the fixed and travel costs, the rejection and tardiness costs of a vaccination appointment are involved. Tang et al. [53] studied a bi-objective vaccination planning problem, providing suggestions on work scheduling, demand assignment, service capacity, and replenishment amount. A weighted-sum, an ϵ-constraint, and a tailored genetic algorithm are adopted to get Pareto solutions. Rahman et al. [50] also optimized a bi-objective problem with multi-level decisions, in which the vaccine loss is addressed via a chance constraint program (CCP).

Equity of vaccination The significance of equity in vaccine distribution was emphasized in Lee et al. [37]. Enayati and Özaltın [22] built a mathematical model to allocate the vaccine among heterogeneous populations to eliminate the influenza outbreak. To access equity, they forced the dispersion of the vaccination rates among all groups to a certain value. Chen et al. [13], Yi and Marathe [63] also discussed equity among *populations*. In another line of research, equity is addressed among *locations*. Chen et al. [11] imposed limitations on the minimum vaccination rate of each facility at each time period to ensure equity. Lim et al. [40] sought to achieve equity by repeatedly running the proposed mathematical model with different groups of candidate locations. Rastegar et al. [51] and Mohammadi et al. [47] adopted vaccine coverage to account for both population and locality equity.

Uncertainty issues The research allowing for the uncertain nature of the vaccine distribution chain is quite limited [19]. To address the uncertain demand, Azadi et al. [6] proposed a two-stage stochastic programming (SP) model for a childhood vaccine administration problem, which is solved by an L-shape method. Azadi et al. [5] derived a CCP for a stochastic distribution problem in low-and middle-income countries. In addition to unstable demand, Yang and Rajgopal [61] also dealt with the uncertainty of travel time, which optimizes the location and routing decisions of mobile clinics. A multi-period modeling method was employed to consider the worst-case scenario and update the decision. Moreover, Yarmand et al. [62] considered a two-phase decision procedure for vaccine allocation to capture the stochastic nature of the epidemic control outcomes (i.e., vaccination coverage). Mohammadi et al. [47] explored the impact of possible disruptions in the vaccine distribution chain via a scenario-based static robust model, which minimizes the total deaths and costs. However, few papers have taken the uncertain supply into account. Lin et al. [41] explored the uncertain production yield and demand of the vaccine supply chain regarding production and procurement decisions. Gilani and Sahebi [26] developed a single-stage data-driven robust optimization model (DDRO) to address uncertain vaccine accessibility. A case study of Iran shows that DDRO performs 21% less conservatively than the classical uncertainty set.

According to the above review, a summary of the most relevant literature is given in Table 1. It can be observed that little attention, except for Gilani and Sahebi [26], has been paid to supply uncertainty in the vaccine distribution field, which is significant given the limited vaccine resources in the early stage. Additionally, none of the above literature takes into account drone delivery for vaccine distribution in rural areas facing difficulties in vaccine storage and transportation. Yet, drone delivery is a promising technology to improve vaccine access and deserves further study. Therefore, our research investigates a drone-based equitable vaccine distribution problem and develops a multi-period two-stage robust model to tackle the supply uncertainty. The model aims to optimize economic and social benefits and jointly determines the facility location, the transportation capacity, and the vaccination reservation plan.

2.2. General location-transportation problem

From the model structure perspective, our research relates to the general two-stage robust location-transportation problem (TRLTP). Cooper [17] was the first to give a general formulation

Table 1
A summary of the most relevant literature.

Authors	Decision level						Multi-period	Drone technology	Equity type		Uncertainty	
	Strategic	Tactical			Operational				Population	Locality	Type	Method
	Location	Service capacity	Vaccine flow	Inventory	Administration	Daily scheduling						
Lim et al. [40]	✓									✓	–	-
Yang and Rajgopal [61]	✓		✓				✓				Demand, travel time	RO
Chen et al. [11]	✓	✓	✓	✓			✓			✓	–	-
Azadi et al. [5]	✓		✓	✓			✓				Demand	CCP
Rastegar et al. [51]	✓		✓	✓			✓		✓	✓	–	-
Tavana et al. [54]	✓		✓	✓			✓		✓	✓	–	-
Mohammadi et al. [47]	✓		✓	✓			✓				Disruption	RO
Li et al. [39]	✓	✓	✓								–	-
Gilani and Sahebi [26]	✓	✓	✓	✓			✓				Accessibility	DDRO
Lai et al. [35]	✓	✓	✓	✓			✓				Demand	SP
Tang et al. [53]	✓					✓	✓				–	-
Zhang et al. [65]	✓					✓					–	-
Habibi et al. [27]	✓		✓	✓							Demand, lead time	Stochastic
Kumar et al. [34]	✓	✓	✓	✓							–	-
Rahman et al. [50]	✓	✓	✓	✓		✓	✓				Vaccine loss	CCP
Balcik et al. [7]			✓						✓	✓	–	-
Yarmand et al. [62]		✓									Vaccination coverage	SP
Jahani et al. [31]		✓		✓			✓				Arrival&service rate	Queue
Georgiadis and Georgiadis [25]		✓	✓	✓		✓	✓				Demand	Rolling-horizon
Fadaki et al. [23]					✓	✓	✓		✓		–	-
Azadi et al. [6]					✓						Demand	SP
Enayati and Özaltın [22]					✓				✓		–	-
Jarumaneeroj et al. [32]					✓	✓	✓				–	-
This paper	✓	✓	✓	✓			✓	✓		✓	Supply	Two-stage RO

of LTP. Crainic and Laporte [18] decomposed transportation planning and operations into three layers: strategic, tactical, and operational planning levels. A location transportation problem usually contains all three levels, which decides the location of open facilities (strategic), the distribution of resources (tactical), and the amount to be transported (operational). Atamtürk and Zhang [4] extended the nominal LTP to a two-stage robust LTP under uncertain demand via a budgeted uncertainty set. They also demonstrated the NP-hard characteristic of TRLTP in the paper. Gabrel et al. [24] adopted Kelley's cutting plane algorithm to exactly solve the problem and reformulated the nonlinear recourse problem as an MILP with a tight bound. Zeng and Zhao [64] solved the same problem by using a new method called the column-and-constraint generation (C&CG) algorithm, which is also a general solution method for two-stage robust optimization problems. Computational results show the efficiency of C&CG as well as its superiority over the benders-style methods. Furthermore, Ardestani-Jaafari and Delage [3] extended the single-period TRLTP to multi-period. To overcome the computational difficulty, they derived six conservative tractable approximations based on the affine adjustment method. Marandi and van Houtum [44] further investigated TRLTP with integer-valued demand and proved that the demand could be relaxed to continuous values without loss of optimality, leveraging the totally unimodal nature of the specific problem. Unfortunately, this characteristic is challenging to generalize to other problems. According to the nature of our problem, the C&CG framework is applied in this study to solve the proposed two-stage robust distribution problem.

3. Model formulation

This section elaborates on the equitable vaccine distribution problem and presents the two-stage robust model.

3.1. Problem description

The problem addressed in this study mainly aims at underdeveloped regions, where there are significant challenges in storing and transporting vaccines in rural areas. Drone delivery is a promising solution that allows for more frequent deliveries, less inventory, and less need for cold chain equipment at health facilities. To this end, a three-tier drone-based vaccine distribution chain is adopted in this research. The schematic illustration of the network is shown in Fig. 1, where the size of the circles represents the population ρ_j of the demand area. Vaccines enter the network at the distribution center such as a central hospital or near that, which is able to meet the requirements for storing the vaccines. Only one distribution center with a given location is involved. Then the vaccines are delivered to the local health facilities via drones. People in demand areas make vaccination appointments based on the vaccine assignment plan, and travel to the health facilities for inoculation according to their appointments. Given the shortage of vaccines, appointment no-shows are not considered. Due to the efficient drone delivery, vaccines are administered the same day they are delivered to the health facilities, which eliminates the need for inventory or wastage at health facilities. Consequently, vaccines are only stored at the distribution center.

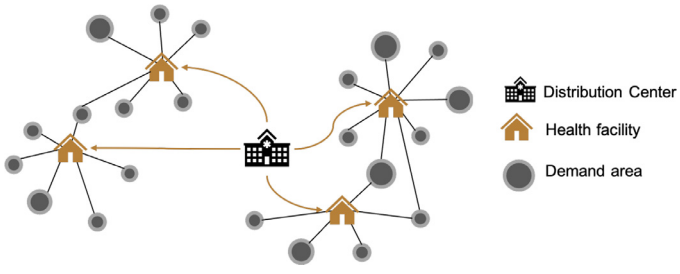

Fig. 1. Illustration of the vaccine distribution chain.

We consider a set I of candidate health facilities and a set J of demand areas. The total scheduled vaccinations at facility i could not exceed its capability $\overline{D}_i$. Let d_i be the distance from the distribution center to facility i, and e_{ij} be the distance from facility i to demand site j. In general, COVID-19 vaccines are delivered on a weekly basis from the government to the distribution center. Based on that, we take one week as the length of the period. A finite time horizon $\mathcal{T} = \{1, 2, \ldots, T\}$ is considered.

Vaccines are assumed to be distributed in single-dose vials. As the two-dose vaccine is considered, let $R = \{1, 2\}$ denote the set of the shot type, and u represent the recommended time interval, which means the second shot should be scheduled u periods after the first shot. Additionally, it is allowed to assign vaccination shots in a demand area to different health facilities at different time periods.

Besides, we assume each drone can only serve one health facility at a time. We set the capacity of a drone to q doses. The endurance of a drone is given as E^T; the facilities out of the range could not be selected. Since this requirement could be pre-checked, we assume all nodes in I are within drone endurance. The total delivery distance of a drone in each time period is restricted to E^D.

3.1.1. Equity of vaccine distribution

Equity is a critical issue for vaccine distribution. Nevertheless, there is not a unified agreement on how to define equity, and various measurements have been taken in the literature. For a summary of these measures in facility location problems, the reader is referred to Marsh and Schilling [45]. One of the widely recognized measures is to consider the difference between the best and the worst performing groups, denoted by

$$\max_i \theta_i - \min_i \theta_i,$$

where θ_i is the performance of group i.

In this research, we define the group performance θ_j as the ratio of v_j the total number of scheduled vaccinations to ρ_j the population of the demand area. We include equity as a constraint to restrict the relative gap between the best and the worst group performance, denoted by $\theta_{\max}$ and $\theta_{\min}$. Then we obtain

$$\frac{\theta_{\max} - \theta_{\min}}{\theta_{\max}} \leq \xi,$$

where ξ is a given parameter of restricted inequity level. Multiplying both sides by $\theta_{\max}$ to linearize the constraint, the complete formulation addressing distribution equity yields

$$\theta_j = \frac{v_j}{\rho_j}, \qquad \forall j \in J, \tag{1a}$$

$$\theta_{\min} \leq \theta_j \qquad \forall j \in J, \tag{1b}$$

$$\theta_{\max} \geq \theta_j \qquad \forall j \in J, \tag{1c}$$

$$\theta_{\max} - \theta_{\min} \leq \xi \theta_{\max}. \tag{1d}$$

3.1.2. Robust problem with uncertain supply

To address the uncertainty of supply, a two-stage robust optimization method is applied. A robust model uses an uncertainty set to characterize the uncertain attributes and focuses on worst-case optimization. One of the most used uncertainty sets to describe the randomness is the so-called budget of uncertainty, see

Bertsimas and Sim [10] and Krumke et al. [33]. The corresponding expression in our model takes the following form:

$$\mathcal{U}_\gamma = \left\{ \boldsymbol{\gamma} \in \mathbb{R}_+^T : \gamma_t \in [a_t, b_t], t \in \mathcal{T}, \text{and} \quad \underline{\Gamma} \le \sum_{t\in\mathcal{T}} \gamma_t \le \overline{\Gamma} \right\}, \tag{2}$$

where γ_t is the uncertain supply arrived at the distribution center at time period t, a_t and b_t are the lower and upper bounds of the uncertain variable γ_t respectively. $\underline{\Gamma}$ and $\overline{\Gamma}$ comprise the bound of the uncertainty budget, restricting the deviation of the total supply. The rationale is that the total supply during the planning horizon (e.g., six weeks) is less fluctuating than the received supply in each period, leading to less conservative solutions.

Assumption 1. In order to get a meaningful uncertainty set, we assume $\sum_{t\in\mathcal{T}} a_t \le \overline{\Gamma}$, $\sum_{t\in\mathcal{T}} b_t \ge \underline{\Gamma}$, and $\underline{\Gamma} \le \overline{\Gamma}$, therefore, $\mathcal{U}_\gamma$ is non-empty.

3.1.3. Decisions and objectives

The two-stage robust approach allows us first to make the first-stage decision and adopt the optimal recourse decision after the uncertainty is confirmed, without encountering infeasibility. Before getting the supply information, we need to decide: (i) $x_i \in \{0, 1\}$ that equals 1 if health facility i is selected and 0 otherwise; (ii) k the number of drones deployed at the distribution center; (iii) D^P_{ijtr} the number of scheduled vaccinations of shot r for demand site j assigned to health facility i at time period t. Given the first-stage decisions, we can reschedule the vaccinations via D^S_{ijtr} according to the realization of vaccine supply, which is the actual number of vaccinations of shot r for demand site j completed at health facility i at time t. If the realized vaccine supply to a facility at time t is less than the scheduled number, the unmet demand will be rescheduled to the coming periods as long as extra vaccines are supplied later. The main purpose of the model is to optimize the first-stage decisions, which take into account the future uncertainty under all situations. In practice, the recourse decisions can be made in a *rolling* manner, meaning that only the recourse decision of the forthcoming period is implemented at the beginning of the period when its uncertainty is realized. Then, based on the newly revealed information in the next period, an optimization problem of rescheduling the vaccinations is solved again, and so on.

Two objectives are considered in our problem, which aims to optimize the social and economic benefits. The social benefit is improved through maximizing the *vaccination profit*, which consists of: (i) the profit of successful vaccinations, (ii) the penalty of vaccination delays, (iii) the penalty of eventually unsatisfied vaccinations as planned, and (iv) the penalty of vaccine wastage due to inefficient use of resources. The economic benefit is enhanced by minimizing the total *cost*, which contains: (i) the setup cost of health facilities, (ii) the deployment cost of drones, (iii) the accessing cost for vaccination, and (iv) the inventory cost. To tackle the two-objective problem, we employ a new coefficient α to adjust the weight of the vaccination profit. Then the problem is integrated into a single-objective form, which maximizes the *total profit*, as shown later in (3a).

3.2. Robust model

A summary of all notation is given in Table 2.

Now, we provide the mathematical model for our equitable pandemic vaccine distribution problem (PVDP). The whole robust counterpart model for our pandemic vaccine distribution problem with uncertain supply can be formulated as

$$\text{(RC-PVDP)} \max_{\boldsymbol{x},\boldsymbol{D^P},k} \; -\left(\sum_{i\in I} C^f x_i + C^k k + \sum_{i\in I}\sum_{j\in J}\sum_{t\in\mathcal{T}}\sum_{r\in R} C^e e_{ij} D^P_{ijtr}\right) + \min_{\boldsymbol{\gamma}\in\mathcal{U}_\gamma} \mathcal{Q}\left(k, \boldsymbol{D^P}, \boldsymbol{\gamma}\right) \tag{3a}$$

$$\text{s.t.} \quad \sum_{r\in R}\sum_{j\in J} D^P_{ijtr} \le \overline{D}_i x_i, \qquad \forall i \in I, t = 1, \dots, T, \tag{3b}$$

$$D^P_{ijt2} = D^P_{ij(t-u)1}, \qquad \forall i \in I, j \in J, t = u+1, u+2, \dots, T, \tag{3c}$$

$$D^P_{ijt2} = \mathcal{D}^S_{ij(t-u)1}, \qquad \forall i \in I, j \in J, t = 1, 2, \dots, u, \tag{3d}$$

$$\sum_{i\in I}\sum_{j\in J}\sum_{r\in R} \frac{D^P_{ijtr}}{q} d_i \le E^D k, \qquad t = 1, 2, \dots, T, \tag{3e}$$

$$v_j = \sum_{r\in R}\sum_{t\in\mathcal{T}}\sum_{i\in I} D^P_{ijtr}, \qquad \forall j \in J, \tag{3f}$$

$$x_i \in \{0, 1\}, \qquad \forall i \in I, \tag{3g}$$

$$k \in \mathbb{Z}^+, \tag{3h}$$

$$D^P_{ijtr} \ge 0, \qquad \forall i \in I, j \in J, r \in R, t = 1, 2, \dots, T, \tag{3i}$$

$$\text{(1a)-(1d)}, \tag{3j}$$

where,

$$\mathcal{Q}\left(k, \boldsymbol{D^P}, \boldsymbol{\gamma}\right) := \max_{\boldsymbol{D^S},\boldsymbol{D^A},\boldsymbol{L}} \; -\sum_{t\in\mathcal{T}} C^l L_t + \alpha\left(\sum_{i\in I}\sum_{j\in J}\sum_{t\in\mathcal{T}}\sum_{r\in R} C^S_r D^S_{ijtr} - \sum_{i\in I}\sum_{j\in J}\sum_{t=1}^{T-1}\sum_{r\in R} C^A_r D^A_{ijtr} - \sum_{i\in I}\sum_{j\in J}\sum_{r\in R} C^U_r D^A_{ijTr} - C^w L_T\right) \tag{4a}$$

$$\text{s.t.} \quad L_t = L_{t-1} + \gamma_t - \sum_{i\in I}\sum_{j\in J}\sum_{r\in R} D^S_{ijtr}, \qquad t = 1, 2, \dots, T, \tag{4b}$$

$$\sum_{i\in I}\sum_{j\in J}\sum_{r\in R} \frac{D^S_{ijtr}}{q} d_i \le E^D k, \qquad t = 1, 2, \dots, T, \tag{4c}$$

$$\sum_{r\in R}\sum_{j\in J} D^S_{ijtr} \le \overline{D_i}, \qquad \forall i \in I, t = 1, 2, \dots, T, \tag{4d}$$

$$D^A_{ijt1} = D^P_{ijt1} + D^A_{ij(t-1)1} - D^S_{ijt1}, \qquad \forall i \in I, j \in J, t = 1, 2, \dots, T, \tag{4e}$$

$$D^A_{ijt2} = D^P_{ijt2} + D^A_{ij(t-1)2} - D^S_{ijt2}, \qquad \forall i \in I, j \in J, t = 1, 2, \dots, u, \tag{4f}$$

$$D^A_{ijt2} = D^S_{ij(t-u)1} + D^A_{ij(t-1)2} - D^S_{ijt2}, \qquad \forall i \in I, j \in J, t = u+1, u+2, \dots, T, \tag{4g}$$

$$D^A_{ijtr}, D^S_{ijtr}, L_t \ge 0, \qquad \forall i \in I, j \in J, r \in R, t = 1, 2, \dots, T. \tag{4h}$$

Table 2
Notation.

Sets	
I	Set of candidate health facilities
J	Set of demand sites
R	$=\{1,2\}$ Set of shot categories
$\mathcal{T}$	$=\{1,2,3\ldots,T\}$ Set of time periods
Parameters	
e_{ij}	Distance from health facility i to demand site j
d_i	Distance from the distribution center to health facility i
ρ_j	Population of demand site j
u	Recommended interval between the two shots
ξ	Restricted deviation level of equity
$\overline{D_i}$	Service capability of health facility i
E^D	The maximum delivery distance of a drone in a time period
q	Capacity of a drone
$\mathcal{D}^S_{ijt1}$	Number of completed vaccinations for the first shot of demand area j assigned to facility i at time t ($t \le 0$) before time horizon
L_0	Initial inventory
γ_t	Supply of vaccine at the distribution center at time t
C^f	Setup cost of a health facility
C^k	Deployment cost of a drone
C^e	Accessing cost of a vaccination
C^l	Inventory cost per vial
C^w	Penalty of wasting a vaccine dose
C^S_r	Profit of a successful vaccination for dose r
C^A_r	Penalty of a service delay of dose r for each time period
C^U_r	Penalty of an ultimately unsatisfied vaccination planned for dose r
Variables	
First-stage	
θ_j	Ratio of the total scheduled vaccinations to the population of demand site j
$\theta_{\min}$	The minimum value of θ_j
$\theta_{\max}$	The maximum value of θ_j
v_j	Total number of scheduled vaccinations of demand site j
D^P_{ijtr}	Number of scheduled vaccinations of demand site j assigned to facility i at time t for shot r
k	Integer variable, number of drones deployed at the distribution center
x_i	Binary variable that equals 1 if health facility i is selected and 0 otherwise
Second-stage	
D^S_{ijtr}	Number of successful vaccinations of demand site j assigned to facility i at time t for shot r
D^A_{ijtr}	Accumulated unsatisfied vaccinations of demand site j assigned to facility i at time t for shot r
L_t	Vaccine inventory at the distribution center at the end of time t

The objective function (3a) seeks to maximize the total profit, containing the fixed cost of health facilities and deploying drones, the accessing cost of vaccinations, and the worst-case profit of the second stage. Constraints (3b) ensure that all vaccinations can only be assigned to the open facilities and the capability of the facilities should be respected. Constraints (3c) and (3d) indicate the second shot should be scheduled u days after the first shot. Constraints (3f) calculate the total number of scheduled vaccinations of each demand site. Constraints (3e) avoid exceeding the delivery capability of drones at the distribution center. The right side approximates the plannable delivery distance and provides an upper bound. Although it is impossible to assign each delivery to multiple drones, this approximation is acceptable in practice since many drone trips (e.g., over 100 in a region) are required per time period. Constraints (3g)–(3i) impose the constraints of the variables.

The objective function (4a) of the second-stage problem consists of the inventory cost and all components of the vaccination profit. Constraints (4b) demonstrate the inventory balance. Similar to constraints (3e), (4c) bound the delivery capability of deployed drones at the distribution center. Constraints (4d) are the limitations on the service capability of the health facilities. The relationship among the initially scheduled vaccinations D^P_{ijtr}, the actual completed vaccinations D^S_{ijtr}, and the accumulated unsatisfied vaccinations D^A_{ijtr} are given in constraints (4e)–(4g). The accumulated unsatisfied vaccinations equal the sum of the vaccinations supposed to be served in this period and the accumulated unsatisfied vaccinations in the previous period minus the vaccinations satisfied in this period. Besides, the rescheduling of the second shot is related to the inoculations of the first shot accomplished u days ago. Constraints (4h) ensure the non-negativity of the variables. From model (4), we can see that the problem has *fixed recourse* (i.e., the coefficients of the second-stage decision variables are not affected by uncertainties). Since the unsatisfied and accumulated vaccinations are associated with penalties, the second-stage problem is always feasible and the problem is *relatively complete* (i.e., it is always possible to find a solution for the recourse problem given the first-stage decisions and uncertainty set).

4. Solution method

Generally, a robust counterpart which is a semi-infinite linear program is NP-hard [9]. It can not be directly solved via an off-the-shelf software like Gurobi in terms of the max-min (min-max) form. Fortunately, our two-stage robust model holds the property of relatively complete and fixed recourse, and the linear inner recourse problem has strong duality. Therefore, according to Theorem 4.6 in Delage [20], the optimal solutions of the robust counterpart problem RC-PVDP can be obtained by only focusing on the vertices of the polyhedron defined by the uncertainty set. As a result, we can use the vertex enumeration method to transform the original two-stage model to a single mixed-integer linear program by adding a copy of the second-stage variables for each vertex. However, this whole enumeration approach will significantly increase the scale of the problem, leading to computational complexities. One effective methodology is referred to as column-and-

constraint generation (C&CG), which is a reduced vertex generation method first introduced by Zeng and Zhao [64]. The algorithm is performed in a master-subproblem framework, where the master problem (MP) is formulated and solved to obtain the first-stage decisions. The subproblem (SP) is used to identify the worst-case uncertain values under the given decisions of the first stage and then add columns and constraints to the master problem *on-the-fly*.

In this section, we first describe the framework of the C&CG algorithm in Section 4.1. Then two tailored algorithms for the subproblem, namely vertex traversal and dual methods, are proposed in Sections 4.2 and 4.3, respectively. With respect to the bilinear character of the dual subproblem, we accordingly give a linearization procedure.

4.1. C&CG framework

Incorporate C&CG algorithm with the proposed RC-PVDP model, and the formulation of the master problem is given as follows.

$$\text{(MP)}\ \Psi := \max\ -(\sum_{i\in I} C^f x_i + C^k k + \sum_{i\in I}\sum_{j\in J}\sum_{t\in\mathcal{T}}\sum_{r\in R} C^e e_{ij} D^P_{ijtr}) + s \tag{5a}$$

$$\text{s.t.}\ \ s \le -\sum_{t\in\mathcal{T}} C^l L^l_t + \alpha(\sum_{i\in I}\sum_{j\in J}\sum_{t\in\mathcal{T}}\sum_{r\in R} C^S_r D^{Sl}_{ijtr} - \sum_{i\in I}\sum_{j\in J}\sum_{t=1}^{T-1}\sum_{r\in R} C^A_r D^{Al}_{ijtr} - \sum_{i\in I}\sum_{j\in J}\sum_{r\in R} C^U_r D^{Al}_{ijTr} - C^w L^l_T), \qquad l = 1,2,\dots,p, \tag{5b}$$

$$L^l_t = L^l_{t-1} + \gamma^l_t - \sum_{i\in I}\sum_{j\in J}\sum_{r\in R} D^{Sl}_{ijtr}, \qquad t = 1,2,\dots,T, l = 1,2,\dots,p, \tag{5c}$$

$$\sum_{i\in I}\sum_{j\in J}\sum_{r\in R}\frac{D^{Sl}_{ijtr}}{q} d_i \le E^D k, \qquad t = 1,2,\dots,T, l = 1,2,\dots,p, \tag{5d}$$

$$\sum_{r\in R}\sum_{j\in J} D^{Sl}_{ijtr} \le \overline{D_i}, \qquad \forall i \in I, t = 1,2,\dots,T, l = 1,2,\dots,p, \tag{5e}$$

$$D^{Al}_{ijt1} = D^P_{ijt1} + D^{Al}_{ij(t-1)1} - D^{Sl}_{ijt1}, \qquad \forall i \in I, j \in J, t = 1,2,\dots,T, l = 1,2,\dots,p, \tag{5f}$$

$$D^{Al}_{ijt2} = D^P_{ijt2} + D^{Al}_{ij(t-1)2} - D^{Sl}_{ijt2}, \qquad \forall i \in I, j \in J, t = 1,2,\dots,u, l = 1,2,\dots,p, \tag{5g}$$

$$D^{Al}_{ijt2} = D^{Sl}_{ij(t-u)1} + D^{Al}_{ij(t-1)2} - D^{Sl}_{ijt2}, \qquad \forall i \in I, j \in J, t = u+1, u+2,\dots,T, l = 1,2,\dots,p, \tag{5h}$$

$$D^P_{ijtr}, D^{Al}_{ijtr}, D^{Sl}_{ijtr}, L^l_t \ge 0, \qquad \forall i \in I, j \in J, r \in R, t = 1,2,\dots,T, l = 1,2,\dots,p, \tag{5i}$$

$$\text{(3b)-(3j)}. \tag{5j}$$

MP attempts to obtain the optimal decisions of the facility location, the drone deployment, and the vaccination reservation plan based on the collection of scenarios identified from the subproblem. Since MP is based on a subset of the uncertainty set $\mathcal{U}_r$, it provides an upper bound (UB) of the complete RC-PVDP problem. The original second-stage variables now feature an extra index l and are denoted by $D^{Al}_{ijtr}, D^{Sl}_{ijtr}, L^l_t$, representing the l_{th} iteration of C&CG algorithm. Similarly, the realization of the uncertain supply becomes γ^l_t. SP is denoted as $\phi := \min_{\gamma\in\mathcal{U}_\gamma} \mathcal{Q}(k, \boldsymbol{D}^P, \boldsymbol{\gamma})$, which helps to provide a lower bound (LB) at each iteration. We compute the relative gap between UB and LB every time after SP is solved. If the gap is less than the given optimality tolerance ϵ, the algorithm terminates. Otherwise, the identified worst scenario and its corresponding variables and constraints are added to MP. MP is a mixed-integer linear program that can be directly solved by an off-the-shelf solve like Gurobi, while the min-max SP will be solved by the vertex traversal and the dual methods illustrated in Sections 4.2 and 4.3 respectively. The detailed process of the C&CG algorithm is described in Algorithm 1.

Algorithm 1: C&CG framework.

1. Initialization: Let $LB = -\infty$, $UB = \infty$, $n = 0$;
2. Solve the deterministic model with fixed γ and obtain the initial solution of $(\hat{k}, \hat{\boldsymbol{D}}^{\boldsymbol{P}}, \hat{\boldsymbol{x}})$. Set UB as the optimal objective value of the solution;
3. Solve the subproblem via the vertex traversal or the dual methods with respect to $(\hat{k}, \hat{\boldsymbol{D}}^{\boldsymbol{P}})$, and find the worst-case scenario.Let $\hat{\phi}$ be the optimal value of the subproblem, and update
$$LB = \max\{LB, -(\sum_{i\in I} C^f \hat{x}_i + C^k \hat{k} + \sum_{i\in I}\sum_{j\in J}\sum_{t\in\mathcal{T}}\sum_{r\in R} C^e e_{ij} \hat{D}^P_{ijtr}) + \hat{\phi}\},$$
and $n = n + 1$;
4. If $(UB - LB)/UB \le \epsilon$, the algorithm terminates; otherwise, add the recourse variables $(\hat{\boldsymbol{D}}^{\boldsymbol{S}}, \hat{\boldsymbol{D}}^{\boldsymbol{A}}, \hat{\boldsymbol{L}})$ and its corresponding constraints associated with the identified worst-case scenario to MP;
5. Solve the MP to get the optimal solution of $(\hat{k}, \hat{\boldsymbol{D}}^{\boldsymbol{P}}, \hat{\boldsymbol{x}})$ and its objective value $\hat{\Psi}$. Update $UB = \hat{\Psi}$. Go to Step 3.

4.2. Subproblem with vertex traversal

In this section, we provide the vertex traversal approach to solve the min-max SP and identify the worst case. The idea is to traverse the elements in the vertex set Ω of the uncertainty set $\mathcal{U}_\gamma$ and identify their minimum value as the optimal solution of SP, i.e., $\hat{\phi} = \min_{\bar{\boldsymbol{\gamma}}\in\Omega} \mathcal{Q}(k, \boldsymbol{D^P}, \bar{\boldsymbol{\gamma}})$. To this end, we introduce Theorem 1 derived from Conforti et al. [16] to generate all vertices.

Theorem 1. *If $\mathcal{U}_\gamma$ is a pointed polyhedron, then $\bar{\boldsymbol{\gamma}}$ is a vertex of $\mathcal{U}_\gamma$ is equivalent to the statement that $\bar{\boldsymbol{\gamma}}$ satisfies at equality of T linearly independent inequalities of $\{a_t \le \gamma_t \le b_t\ \forall t \in \mathcal{T}$, and $\underline{\Gamma} \le \sum_{t\in\mathcal{T}} \gamma_t \le \overline{\Gamma}\}$.*

Obviously, there are $T + 1$ groups of constraints linearly independent of each other when $T \ge 2$. And the two constraints within each group are linearly dependent. We have to select T out of $T + 1$ constraint groups and choose one constraint within each group to get all vertices. The feasibility should also be satisfied. The procedure to get the vertex set Ω is displayed in Algorithm 2. There are less than $(T + 1)2^T$ vertices in $\mathcal{U}_\gamma$. Then, we solve the maximization problem $\mathcal{Q}(k, \boldsymbol{D^P}, \bar{\boldsymbol{\gamma}})$ traversing all $\bar{\boldsymbol{\gamma}} \in \Omega$ at each iteration and figure out the worst case as the result of SP. Compared to the basic whole vertex enumeration method, C&CG with vertex traversal still needs to generate all vertices, but does not need to add them to the master problem at one time, which significantly improves computational efficiency.

4.3. Subproblem with dual method

We now provide another approach that attempts to tackle the subproblem via the dual method instead of the vertex traversal in

Algorithm 2: Procedure to get the vertex set of $\mathcal{U}_\gamma$.

Data: $\underline{\Gamma}, \overline{\Gamma}, a_t, b_t \forall t \in \mathcal{T}$
Result: Vertex set Ω
Initialization: $n = 0$, $\Omega = \varnothing$;
Step 1: select constraint groups $1 \sim T$, enumerate all 2^T scenarios:
  Let $\bar{\gamma}_t = a_t$ or b_t, $\forall t \in \mathcal{T}$, generate all 2^T basic solutions $\tilde{\boldsymbol{\gamma}}$;
  Check the feasibility of $\tilde{\boldsymbol{\gamma}}$: if $\underline{\Gamma} \le \sum_t \bar{\gamma}_t \le \overline{\Gamma}$, add $\tilde{\boldsymbol{\gamma}}$ to Ω.Step 2 : select a constraint group n from 1 to T, use the other T constraint groups to enumerate all $T2^T$ scenarios:
  Let $\bar{\gamma}_t = a_t$ or $b_t, \forall t \in \mathcal{T}\backslash n$, $\bar{\gamma}_n = \overline{\Gamma} - \sum_{t\in\mathcal{T}\backslash n} \bar{\gamma}_t$ or $\underline{\Gamma} - \sum_{t\in\mathcal{T}\backslash n} \bar{\gamma}_t$, generate all $T2^T$ basic solutions $\boldsymbol{\gamma}$;
  Check the feasibility of $\tilde{\boldsymbol{\gamma}}$: if $a_n \le \bar{\gamma}_n \le b_n$, add $\tilde{\boldsymbol{\gamma}}$ to Ω.Return the final Ω.

the C&CG framework. Given $\hat{k}, \hat{\boldsymbol{D}}^{\boldsymbol{P}}$ obtained from MP, we take the dual to convert the min-max SP to a min-min problem, which can be regarded as a minimization problem. Let $\boldsymbol{\lambda}$, $\boldsymbol{\delta}$, $\boldsymbol{\beta}$ be the dual variables for constraints (4b)–(4d), $\boldsymbol{\pi}$ for (4e), and $\boldsymbol{\eta}$ for (4f)–(4g), respectively. The resulting dual formula of the inner maximization problem $\mathcal{Q}(\hat{k}, \hat{\boldsymbol{D}}^{\boldsymbol{P}}, \hat{\boldsymbol{\gamma}})$ with fixed $\hat{\boldsymbol{\gamma}}$ is written as

DSP$(\hat{k}, \hat{\boldsymbol{D}}^{\boldsymbol{P}}, \hat{\boldsymbol{\gamma}})$:

$$\min_{\boldsymbol{\lambda},\boldsymbol{\delta},\boldsymbol{\beta},\boldsymbol{\pi},\boldsymbol{\eta}} \; -(\hat{\gamma}_1 + L_0)\lambda_1 - \sum_{t=2}^{T} \hat{\gamma}_t \lambda_t + \sum_{t=1}^{T} E^D \hat{k} \delta_t + \sum_{i\in I}\sum_{t=1}^{T} \overline{D}_i \beta_{it} - \sum_{i\in I}\sum_{j\in J}\sum_{t=1}^{T} \hat{D}^P_{ijt1}\pi_{ijt} - \sum_{i\in I}\sum_{j\in J}\sum_{t=1}^{u} \hat{D}^P_{ijt2}\eta_{ijt}, \tag{6a}$$

$$\text{s.t.} \;\; \lambda_t - \lambda_{t+1} \le C^I, \qquad t = 1, 2, \ldots, T-1, \tag{6b}$$

$$\lambda_T \le C^I, \tag{6c}$$

$$\lambda_t - \delta_{it} - \beta_{it} + \pi_{ijt} - \eta_{ij(t+u)} \le 0, \qquad \forall i \in I, j \in J, t = 1, 2, \ldots, T-u, \tag{6d}$$

$$\lambda_t - \delta_{it} - \beta_{it} + \pi_{ijt} \le 0, \qquad \forall i \in I, j \in J, t = T-u+1, T-u+2, \ldots, T, \tag{6e}$$

$$\lambda_t - \delta_{it} - \beta_{it} + \eta_{ijt} \le 0, \qquad \forall i \in I, j \in J, t = 1, 2, \ldots, T, \tag{6f}$$

$$\pi_{ijt} - \pi_{ij(t+1)} \le \alpha C^A_1, \qquad \forall i \in I, j \in J, t = 1, 2, \ldots, T-1, \tag{6g}$$

$$\pi_{ijT} \le \alpha C^U_1, \qquad \forall i \in I, j \in J, \tag{6h}$$

$$-\eta_{ij(t+1)} + \eta_{ijt} \le \alpha C^A_2, \qquad \forall i \in I, j \in J, t = 1, 2, \ldots, T-1, \tag{6i}$$

$$\eta_{ijT} \le \alpha C^U_2, \qquad \forall i \in I, j \in J, \tag{6j}$$

$$\delta_t, \beta_{it} \ge 0, \qquad \forall i \in I, j \in J, t = 1, 2, \ldots, T. \tag{6k}$$

Let $\mathcal{V}$ denote the feasible region of DSP$(\hat{k}, \hat{\boldsymbol{D}}^{\boldsymbol{P}}, \hat{\boldsymbol{\gamma}})$, which is a bounded non-empty polyhedron.

Next, we equivalently transform the complete min-max SP into a single-level minimization problem as

DSP$(\hat{k}, \hat{\boldsymbol{D}}^{\boldsymbol{P}})$:

$$\min_{\boldsymbol{\lambda},\boldsymbol{\delta},\boldsymbol{\beta},\boldsymbol{\pi},\boldsymbol{\eta},\boldsymbol{\gamma}} \; -(\gamma_1 + L_0)\lambda_1 - \sum_{t=2}^{T} \gamma_t \lambda_t + \sum_{t=1}^{T} E^D \hat{k} \delta_t + \sum_{i\in I}\sum_{t=1}^{T} \overline{D}_i \beta_{it} - \sum_{i\in I}\sum_{j\in J}\sum_{t=1}^{T} \hat{D}^P_{ijt1}\pi_{ijt} - \sum_{i\in I}\sum_{j\in J}\sum_{t=1}^{u} \hat{D}^P_{ijt2}\eta_{ijt} \tag{7a}$$

$$\text{s.t.} \;\; \text{(6b)-(6k)}, \tag{7b}$$

$$a_t \le \gamma_t, \qquad t = 1, 2, \ldots, T, \tag{7c}$$

$$b_t \ge \gamma_t, \qquad t = 1, 2, \ldots, T, \tag{7d}$$

$$\sum_{t\in\mathcal{T}} \gamma_t \ge \underline{\Gamma}, \tag{7e}$$

$$\sum_{t\in\mathcal{T}} \gamma_t \le \overline{\Gamma}. \tag{7f}$$

4.3.1. Reformulation

Due to the existence of the bilinear term $\gamma_t\lambda_t$ in the objective function, where γ_t and λ_t are both continuous variables, DSP$(\hat{k}, \hat{\boldsymbol{D}}^{\boldsymbol{P}})$ is a nonlinear program that cannot be efficiently solved by existing optimization solvers (e.g., Gurobi). To this end, we provide a reformulation method to recast this bilinear constraint to a linear formulation.

We first implement Algorithm 1 to enumerate the vertex set Ω of the uncertainty set $\mathcal{U}_\gamma$. Let $\tilde{\boldsymbol{\gamma}} = [\bar{\gamma}_1, \bar{\gamma}_2, \ldots, \bar{\gamma}_T]$ denote a vertex in Ω, and $G_t = \{g_1, g_2, \ldots, g_n\}$ be the set of all possible values of $\bar{\gamma}_t$, $\forall \tilde{\boldsymbol{\gamma}} \in \Omega$. For example, if $T = 2$ and there are two vertices of $\mathcal{U}_\gamma$ which are $\tilde{\boldsymbol{\gamma}}^1 = [1, 2]$, $\tilde{\boldsymbol{\gamma}}^2 = [1, 3]$, then $\bar{\gamma}_1$ can only take value 1 and $\bar{\gamma}_2$ could be 2 or 3, $\forall \tilde{\boldsymbol{\gamma}} \in \Omega$. Accordingly, $G_1 = \{1\}$, $G_2 = \{2, 3\}$. Then, we introduce the following lemma.

Lemma 1. *There exists an optimal solution* $(\boldsymbol{\lambda}^*, \boldsymbol{\delta}^*, \boldsymbol{\beta}^*, \boldsymbol{\pi}^*, \boldsymbol{\eta}^*, \boldsymbol{\gamma}^*)$ *of DSP*$(\hat{k}, \hat{\boldsymbol{D}}^{\boldsymbol{P}})$ *such that* $\boldsymbol{\gamma}^*$ *is a vertex of* $\mathcal{U}_\gamma$ *and* $\gamma_t^* \in G_t$, $\forall t = 1, 2, \ldots, T$.

Proof. Let E and Ω be the vertex sets of $\mathcal{V}$ and $\mathcal{U}_\gamma$ respectively. As DSP$(\hat{k}, \hat{\boldsymbol{D}}^{\boldsymbol{P}})$ is a bilinear problem and both $\mathcal{V}$ and $\mathcal{U}_\gamma$ are bounded polyhedra, then there exists an optimal solution $(\boldsymbol{\lambda}^*, \boldsymbol{\delta}^*, \boldsymbol{\beta}^*, \boldsymbol{\pi}^*, \boldsymbol{\eta}^*, \boldsymbol{\gamma}^*)$ such that $(\boldsymbol{\lambda}^*, \boldsymbol{\delta}^*, \boldsymbol{\beta}^*, \boldsymbol{\pi}^*, \boldsymbol{\eta}^*)$ is a vertex of $\mathcal{V}$ and $\boldsymbol{\gamma}^*$ is a vertex of $\mathcal{U}_\gamma$ [29]. Accordingly, $\gamma_t^* \in G_t$, $\forall t = 1, 2, \ldots, T$. □

Based on the above lemma, we reformulate the nonlinear program $(\hat{k}, \hat{\boldsymbol{D}}^{\boldsymbol{P}})$ as a mixed-integer linear program, which could be efficiently solved by off-the-shelf software like Gurobi based on the following Theorem.

Theorem 2. *The nonlinear programming DSP*$(\hat{k}, \hat{\boldsymbol{D}}^{\boldsymbol{P}})$ *can be recast as follows:*

LDSP$(\hat{k}, \hat{\boldsymbol{D}}^{\boldsymbol{P}})$*:*

$$\min_{\boldsymbol{\lambda},\boldsymbol{\delta},\boldsymbol{\beta},\boldsymbol{\pi},\boldsymbol{\eta},\boldsymbol{\gamma}} \; -L_0\lambda_1 - \sum_{t=1}^{T} h_t + \sum_{t=1}^{T} E^D \hat{k} \delta_t + \sum_{i\in I}\sum_{t=1}^{T} \overline{D}_i \beta_{it} - \sum_{i\in I}\sum_{j\in J}\sum_{t=1}^{T} \hat{D}^P_{ijt1}\pi_{ijt} - \sum_{i\in I}\sum_{j\in J}\sum_{t=1}^{u} \hat{D}^P_{ijt2}\eta_{ijt} \tag{8a}$$

$$\text{s.t.} \;\; \text{(6b)-(6k)}, \tag{8b}$$

$$z_{tg} = 1 \Rightarrow h_t = g\lambda_t, \qquad \forall t \in \mathcal{T}, \forall g \in G_t, \tag{8c}$$

$$\sum_{g\in G_t} z_{tg} = 1, \qquad \forall t \in \mathcal{T}, \tag{8d}$$

$$\sum_{t\in\mathcal{T}}\sum_{g\in G_t} z_{tg} g \geq \underline{\Gamma}, \tag{8e}$$

$$\sum_{t\in\mathcal{T}}\sum_{g\in G_t} z_{tg} g \leq \overline{\Gamma}, \tag{8f}$$

$$z_{tg} \in \{0,1\} \qquad \forall t \in \mathcal{T}, \forall g \in G_t, \tag{8g}$$

where (8c) are indicator constraints, in which the linear equality holds when $z_{tg} = 1$.

Proof. Let h_t substitute for the bilinear term $\gamma_t \lambda_t$ in (7a). Then we eliminate this nonlinear equation $h_t = \gamma_t \lambda_t$ by introducing a new binary z_{tg} that equals 1, if g is chosen to be the optimal value of γ_t, and 0 otherwise. Consequently, we obtain constraints (8d), (8g), and

$$h_t = \begin{cases} 0, & \text{if } z_{tg} = 0 \\ g\lambda_t, & \text{if } z_{tg} = 1 \end{cases}, \forall t \in \mathcal{T}, g \in G_t. \tag{9}$$

Although the big-M method is a common approach to deal with the type of nonlinear formulation of (9), which contains a binary variable, it is not appropriate for our dual problem. Because a rigorous value of big-M is difficult to choose, since there are no valid bounds on the gap of limit values of λ_t. The use of an arbitrary big value will reduce the efficiency of solving the problem and lead to the risk of incorrect results. Alternatively, we use the so-called *indicator constraints* to reformulate constraints (9) as constraints (8c), which can be directly implemented in the optimization solvers like Gurobi. In addition, since $g \in G_t$ is a possible value of $\bar{\gamma}_t$ in a vertex, constraints (7c) and (7d) are inherently guaranteed. Constraints (7e) and (7f) and are substituted by (8e) and (8f) respectively. At this point, the proof has been completed. □

5. Case study

In this section, we first describe the settings of our numerical study and introduce the data of Linshui County in Sichuan Province, PR China. We conduct computational experiments to test the efficiency of the proposed C&CG algorithms with the vertex traversal and the dual methods, respectively. Then we use the case study to evaluate the performance of the nominal and robust problems and analyze the impact of important coefficients. In addition, the significance of considering equity in vaccine distribution is also illustrated.

All numerical experiments in this research are implemented in Python language, using Gurobi (v9.0.1) to solve the mathematical programs. All tests are performed on a Macbook Pro with a 2 GHz Intel i5 CPU and 16 G memory running the mac OS operating system.

5.1. Data generation

The procedure to generate the data is described as follows. The capacity q and the endurance E^T of a drone are set to 25 vials and 25 kilometers, respectively, while E^D the total delivery distance in a period (one week) is capped at 7×20 times E^T, that is 3500 kilometers. The recommended interval between two shots u is three weeks. We consider a default planning horizon T of 6 weeks and limit ξ the restricted deviation of vaccination equity to 0.1. Moreover, the deployment cost C^k of a drone is fixed at 6000 US dollars, which is the reference price from the business-to-business e-commerce website b2b.baidu.com, and the setup cost

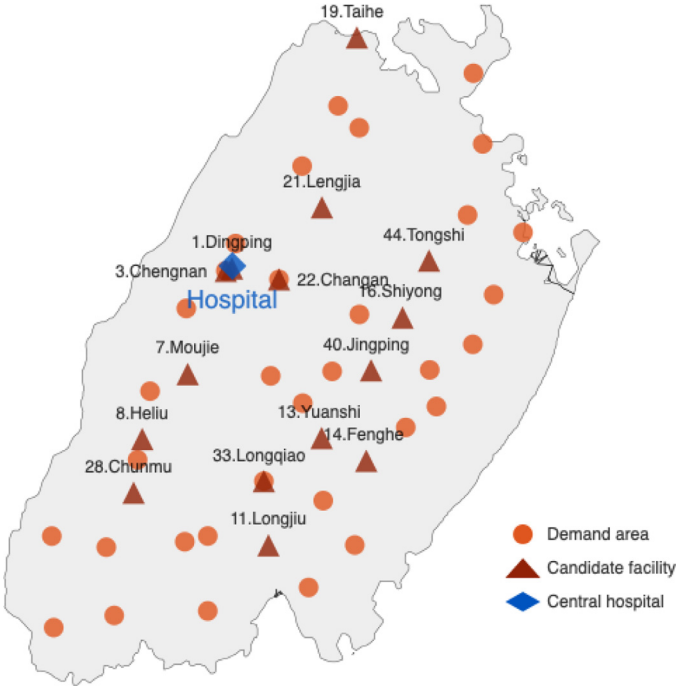

Fig. 2. Map of Linshui County.

C^f of a health facility is by default set to 6000 dollars. We set the accessing cost $C^e = 0.2$, and the inventory cost $C^l = 0.2$. As for the coefficients related to the vaccination profit, we have the penalty of vaccine wastage $C^w = 2$. Since two-shot inoculation is scheduled, i.e., $R = \{1, 2\}$, we accordingly set the profit of successful vaccinations $\boldsymbol{C^S} = (3, 4)$, the penalty of vaccination delays $\boldsymbol{C^A} = (1, 2)$, and the penalty of eventually unsatisfied vaccinations $\boldsymbol{C^U} = (2, 3)$ respectively. The weight coefficient α is set to 5 by default.

Regarding the uncertain supply, we use the nominal supply denoted by $\boldsymbol{\gamma'}$ as the baseline. Let ϵ indicate the deviation of the supply uncertainty level, taking 0.7 as the default value. Accordingly, $a_t = (1-\epsilon)\gamma'_t$ and $b_t = (1+\epsilon)\gamma'_t$. Note that both a_t and b_t are forced to be integer values. For the budget of total supply, we assume $\overline{\Gamma} = \max_t\{a_t + \sum_{t'\in\mathcal{T}\setminus t} b_{t'}\}$ and $\underline{\Gamma} = \min_t\{b_t + \sum_{t'\in\mathcal{T}\setminus t} a_{t'}\}$ to allow for a moderate budget which cuts off the most extreme situation.

Except for the test of algorithm performance in Section 5.2, which is conducted based on the randomly generated instances, all the experiments are performed through the data of Linshui County. Linshui is located in the remote area of Sichuan Province, PR China with many mountainous areas and 45 sub-districts under its jurisdiction. The name and population of these villages are given in Table 7 in the Appendix, where the population data is obtained from the 2021 census conducted by Guang'an Bureau of Statistics. The central hospital is identified as the vaccine distribution center. According to the actual situation of medical infrastructure in each area, 15 of these villages are chosen as the candidate facilities. The map of Linshui County along with the above three types of sites is displayed in Fig. 2. The coordinates of all locations are obtained from Google Maps, then the Euclidean distance is calculated to get d_i and e_{ij}. The service capabilities $\overline{D}_i$ are classified into three levels as [3000, 7000, 10,000] given in Table 7. The nominal value of vaccine supply is taken from Linshui's actual supply of six weeks between May and July 2021, specified as $\boldsymbol{\gamma'} = (25,200, 10,000, 64,948, 44,400, 25,706, 37,998)$. The data is collected from the announcement of Linshui Center for Disease Control and Prevention.

Table 3
Algorithm efficiency of C&CG algorithms on RC-PVDP.

$\|I\|$	$\|J\|$	T	Vertex	CPU time(s)						Gap(%)		Iter
				C&CG with traversal			C&CG with dual					
				total	MP	SP	total	MP	SP	total	SP	
10	15	4	20	8.2	0.8	7.4	1.2	0.8	0.4	85.8	94.7	2.0
		5	41	21.9	1.3	20.6	5.2	1.3	3.9	76.4	81.3	2.3
		6	72	43.9	1.8	42.1	3.9	1.8	2.1	91.1	95.0	2.3
	30	4	20	17.5	2.1	15.5	2.7	2.0	0.7	84.6	95.6	2.3
		5	43	48.9	4.6	44.3	9.7	4.7	5.1	80.1	88.5	2.7
		6	72	96.1	6.1	90.0	9.7	6.2	3.4	90.0	96.2	2.7
	50	4	23	25.9	2.7	23.2	3.6	2.7	0.9	86.2	96.1	2.0
		5	42	78.0	7.6	70.5	11.1	7.5	3.6	85.8	94.9	2.7
		6	72	159.3	14.9	144.4	19.6	14.9	4.6	87.7	96.8	2.7
20	30	4	21	54.7	11.9	42.8	13.4	11.8	1.6	75.5	96.3	3.9
		5	42	111.2	12.4	98.8	17.2	12.5	4.7	84.6	95.2	3.5
		6	72	190.9	12.2	178.7	16.2	12.2	4.0	91.5	97.8	3.0
	50	4	20	98.3	23.3	75.0	25.7	23.2	2.5	73.8	96.6	4.2
		5	42	186.1	21.5	164.6	28.4	21.5	6.8	84.7	95.8	3.6
		6	72	325.5	22.0	303.5	28.8	22.5	6.3	91.1	97.9	3.0
	80	4	20	173.8	55.4	118.4	59.9	55.6	4.3	65.6	96.4	4.1
		5	43	337.5	48.4	289.1	64.1	48.4	15.7	81.0	94.6	3.4
		6	72	596.3	55.0	541.3	63.9	54.3	9.6	89.3	98.2	3.2
30	50	4	21	179.9	59.6	120.3	63.2	59.4	3.8	64.9	96.8	4.1
		5	41	355.2	85.4	269.8	95.6	86.5	9.1	73.1	96.6	3.6
		6	72	591.5	94.6	496.9	101.6	93.6	8.1	82.8	98.4	3.2
	80	4	21	418.9	246.9	172.1	256.4	251.4	5.0	38.8	97.1	3.8
		5	40	741.9	332.6	409.3	346.2	334.3	11.9	53.3	97.1	3.6
		6	72	1075.7	285.9	789.8	295.4	283.6	11.8	72.5	98.5	3.3
	100	4	21	750.8	493.8	257.0	503.5	496.3	7.3	32.9	97.2	4.7
		5	42	1044.2	516.4	527.8	521.5	506.4	15.1	50.1	97.1	3.6
		6	72	1639.3	625.5	1013.8	616.8	602.5	14.3	62.4	98.6	3.3
Average				347.1	112.8	234.3	117.9	111.8	6.2	75.4	95.8	3.2

5.2. Comparison of algorithm performance

This section compares the performance of the proposed C&CG algorithms with the vertex traversal and the dual methods. We run 27 groups of experiments using different values of $|I|$, $|J|$, and T. Ten instances are randomly generated under each setting, and the average values are taken for performance analysis. Candidate health facilities and demand sites are randomly drawn from a uniform distribution $U(0, 50)$. The coordinate of the distribution center is set to (25,25). We independently and uniformly generate ρ_j from (1,5), γ_t from (20,000, 70,000), and $\bar{D}_i$ from (1000, 10,000).

The results are reported in Table 3, where column Vertex represents the total number of vertices of the uncertainty set $\mathcal{U}_\gamma$ and column Iter indicates the iteration times between the master and the subproblem. The computational time to solve the complete, master, and sub problems is provided in total, MP, and SP, respectively. Gap(%) illustrates the relative gap of CPU time between the two algorithms. Since both methods share the same C&CG framework, they converge in the same number of iterations. All instances can be solved optimally within a small number of iterations with an average of 3.2. Moreover, we can observe that all CPU time rises with the problem size in general. As expected, the values of the master problem of the two algorithms are nearly the same. For subproblems, the dual method consumes very little CPU time even for the largest instance, while the traversal method takes over one thousand seconds.

On average, C&CG with the dual approach outperforms the traversal method in computational efficiency in total, which mainly results from the resolution for subproblem. These advantages become more prominent as the scale of the problem increases. C&CG with the dual method can efficiently solve all instances to optimality. Based on the above results, C&CG with the dual method is adopted for our further analysis.

5.3. Impact of the uncertainty

From this section, the models are applied to the case study of Linshui County. We compare the worst-case results of the deterministic model and the robust model when the uncertain level ϵ varies from 0 to 0.9, with the weight coefficient of vaccination profit $\alpha \in \{0.5, 1, 5, 20\}$. The detailed results are given in Table 4, where the rows with $\epsilon = 0$ depict the solutions under the deterministic situations. To show the result of the optimal decisions, we use X_{sum} to represent the total number of selected facilities (i.e., $X_{sum} = \sum_{i\in I} x_i$), k is the number of deployed drones, and D^P_{sum} provides the total number of scheduled vaccinations (i.e., $D^P_{sum} = \sum_{i\in I}\sum_{j\in J}\sum_{r\in R}\sum_{t\in\mathcal{T}} D^P_{ijtr}$). As for the calculation of the profit, we set the instance with $\alpha = 5$, $\epsilon = 0.5$ for the robust model as the benchmark, and other results are computed by the percentage increase compared to its total profit. The column Gap provides the difference ratio value of the robust and deterministic model.

We first analyze the impact of uncertainty on the decision structure. The optimal decision of the deterministic model (depicted by $\epsilon = 0$) is fixed under a given α independent of the uncertainty level ϵ. As for the robust model, we see that when the weight coefficient α is small (e.g., $\alpha = 0.5$ or 1), the number of opened facilities and deployed drones reduces with the rise of the uncertain level ϵ. While the trend turns out the opposite as α becomes larger (e.g., $\alpha = 5$ or 20). This implies when the decision-maker cares about the economic benefit (lower α), it is reason-

Table 4
Results of different uncertainty levels.

α	ϵ	X_{sum}	k	D^P_{sum}	Total profit ratio		
					Robust	Deterministic	Gap
0.5	**0**	**11**	**8**	**144,548**	**−0.89**	**−0.89**	**0**
	0.1	11	8	140,434	−1.02	−1.07	0.05
	0.3	10	7	130,978	−1.27	−1.48	0.21
	0.5	10	6	119,596	−1.53	−1.89	0.36
	0.7	10	6	110,510	−1.81	−2.29	0.48
	0.9	8	5	98,901	−2.07	−2.7	0.63
1	**0**	**11**	**8**	**144,548**	**0.01**	**0.01**	**0**
	0.1	11	8	139,887	−0.19	−0.27	0.08
	0.3	10	7	129,325	−0.61	−0.87	0.26
	0.5	10	6	117,496	−1.04	−1.49	0.45
	0.7	10	6	106,889	−1.47	−2.1	0.63
	0.9	8	5	94,549	−1.9	−2.71	0.81
5	**0**	**11**	**8**	**144,548**	**1.81**	**1.81**	**0**
	0.1	11	8	139,377	1.46	1.34	0.12
	0.3	12	8	128,982	0.74	0.33	0.41
	0.5	12	10	118,536	0	−0.69	0.69
	0.7	14	11	107,250	−0.76	−1.71	0.95
	0.9	14	11	95,176	−1.53	−2.74	1.21
20	**0**	**12**	**8**	**144,548**	**2.45**	**2.45**	**0**
	0.1	15	8	139,252	2.03	1.92	0.11
	0.3	15	8	128,670	1.22	0.76	0.46
	0.5	15	10	118,057	0.4	−0.41	0.81
	0.7	15	12	106,906	−0.45	−1.58	1.13
	0.9	15	12	94,674	−1.33	−2.75	1.42

able to decline the investments to save cost, since the vaccination profit cannot dominate the cost when the vaccine supply is too unpredictable. However, when social benefit really matters, more facilities and drones are required in the robust model to accelerate the vaccination procedure and improve the total profit, coping with the increased uncertainty. An interesting observation is that the total number of scheduled vaccinations inevitably decreases with the growth of ϵ, even with large values of α. This is because no matter how important the vaccination profit is, planning additional vaccination will incur higher waste penalties or inventory costs in terms of the turbulent supply. Therefore, it is suggested to plan fewer vaccinations to diminish the higher uncertainty.

Another effect is reflected in profits. The decline in total profits is the price of the increased supply uncertainty in both problems. Whereas, the robust model is less affected compared to the deterministic model. Besides, the robust model performs better on the total profit, and this advantage rises as the uncertainty level grows. To better illustrate this observation and further investigate the impacts on the components of the total profit, we plot the detailed profit ratios with $\alpha = 5$ by varying ϵ in Fig. 3. The lines depicting the total and the vaccination profits of the robust model lie over those of the deterministic model, declining much flatter, which verifies our former conclusion. Meanwhile, the cost remains steady at −0.01 in the deterministic model, while it shows a tortuous upward trend in the robust model. This is owing to the interaction of the increased fixed cost and decreased accessing cost. In addition, the change caused by supply uncertainty in cost (< 0.04) is relatively small compared to the profits (> 1), indicating that sometimes a small rise in the nominal cost can lead to a substantial drop in the worst-case profit. It is beneficial for decision-makers to account for future supply variation when determining the facility locations as well as their capacity and vaccination reservation plan in the first planning stage.

5.4. Sensitivity analyses

In this section, we leverage the robust model to provide the sensitivity analyses of the following three parameters: the weight coefficient α, the wastage penalty C^w, and the facility fixed cost C^f. The analyses mainly focus on two aspects: (i) the structure of the optimal decisions, comprising the number of selected facilities, deployed drones, and total scheduled vaccinations; (ii) the normalized profits, including the total profit, the vaccination profit, and the revised cost (- cost is used to transform the cost into profit version). The total profit is normalized through dividing the objective value by $1 + \alpha$, and the vaccination profit is calculated without α.

5.4.1. Impact of the weight coefficient α

The impact of the vaccination weight coefficient α on the optimal decisions is illustrated in Fig. 4. The larger the α, the more significant the social benefit. The growing of α leads to more investment in facilities and drones. This is because additional facilities and drones are required for quicker delivery to improve the vaccination profit, as the cost becomes less critical in the objective function. On the contrary, the number of total scheduled vaccinations shows a declining trend, which is quite counter-intuitive. The reason behind this is complicated, as the cost of inventory, the penalty of wastage and injection delay, and the profit of completed vaccinations are all tied to the scheduled vaccinations, compounding the impact on the final result. One of the critical factors lines in inventory cost. The optimal decision of the robust problem in

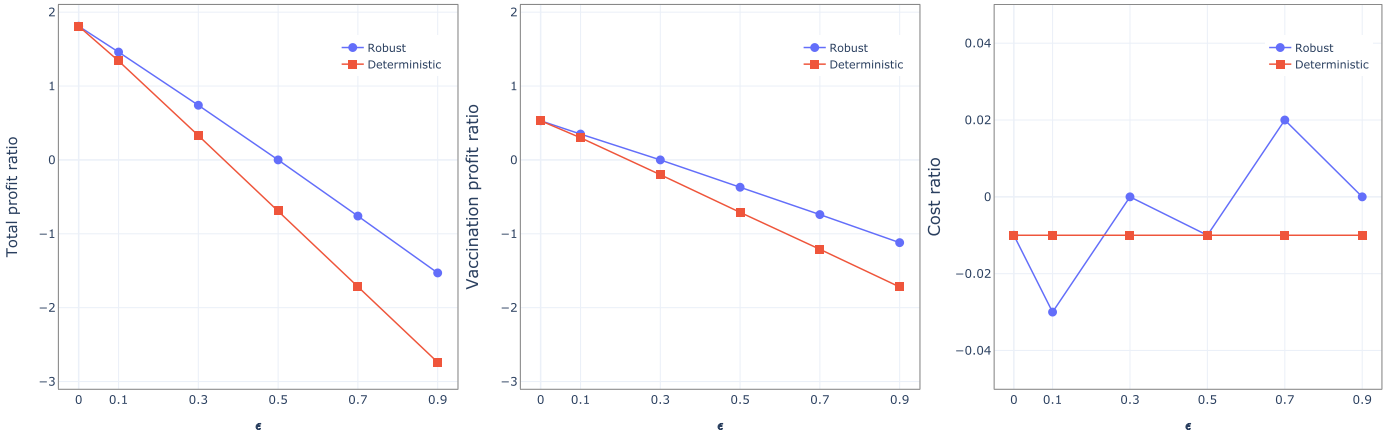

Fig. 3. Comparative results on profits under different uncertainty levels $\epsilon \in [0, 0.9]$ with $\alpha = 5$.

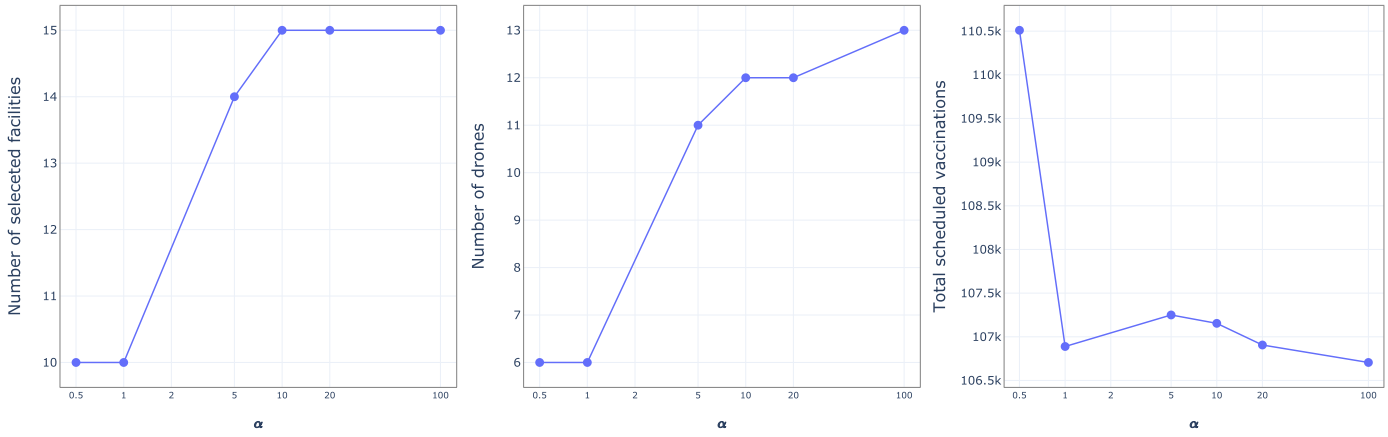

(a) Number of selected facilities (b) Number of drones (c) Total scheduled vaccinations

Fig. 4. Impact of the weight coefficient α on the optimal decisions.

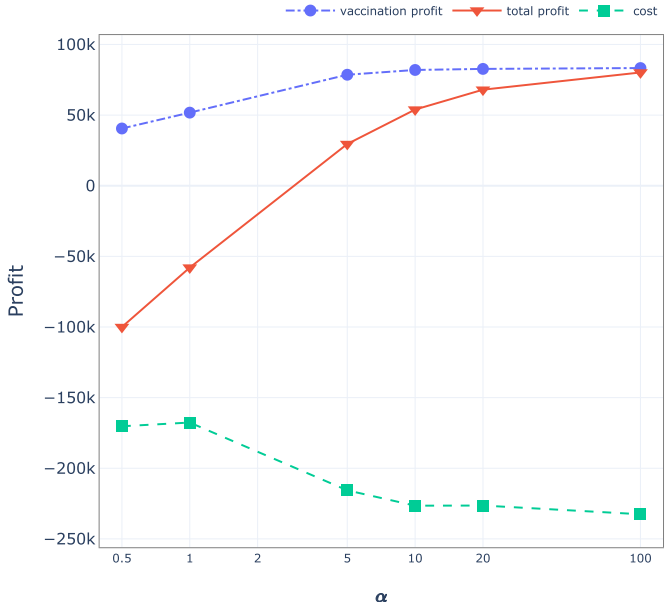

Fig. 5. Impact of the weight coefficient α on the profits.

this study is to balance all scenarios of vaccine supply, making the profit of the worst case more acceptable. Except for the inventory cost, all the other costs are nearly the same under all scenarios. Thus, as the cost becomes more prominent, more vaccinations are scheduled to lower the inventory cost for the worst case. Overall, the decisions are sensitive to α, but the number of scheduled vaccinations is inconsistent with the changes in α.

Figure 5 gives the information on the impact of α on the profits. As we put more emphasis on the social benefit, which is manifested by the growing of α, the vaccination profit goes up while the cost goes down as expected. Consequently, the total profit rises throughout. It is noted that when α reaches 100, the total profit is almost equal to the vaccination profit. When α is extremely small, the total profit is supposed to approach the value of - cost. Hence, the impact of α on the social and economic benefits is significant.

5.4.2. Impact of the waste penalty C^w

Figure 6 presents the change of the solution structure with $C^w \in \{0, 1, 2, 3, 4\}$. The number of opened facilities, distributed drones, and scheduled vaccinations increases as expected, which diminishes the waste by speeding up the delivery process and accomplishing more vaccinations. Figure 7 shows a monotone downward trend in the total profit and the vaccination profit with the growing of C^w, which agrees with our intuition. Although the revised

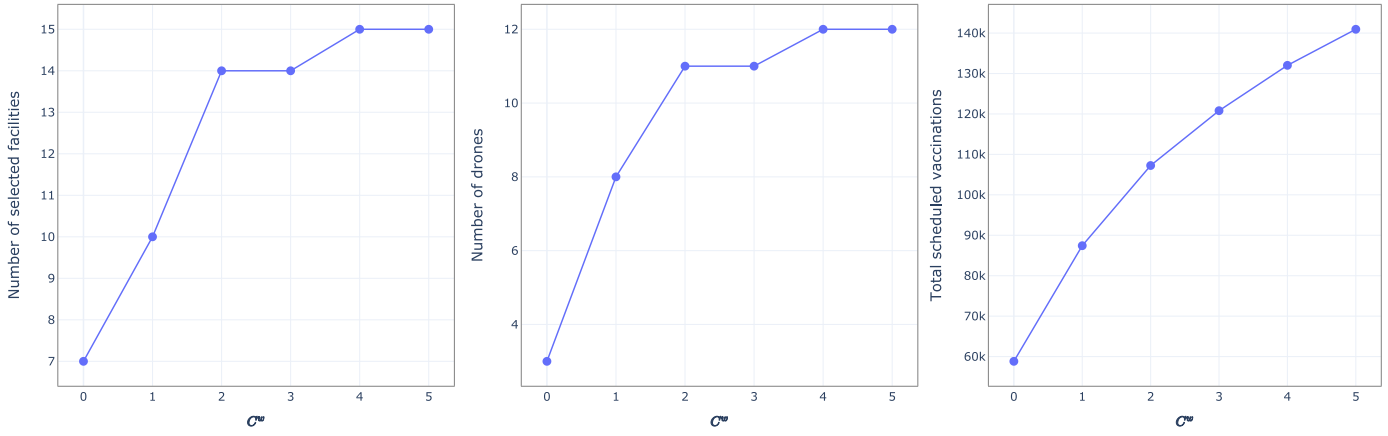

(a) Number of selected facilities (b) Number of drones (c) Total scheduled vaccinations

Fig. 6. Impact of the wastage penalty C^w on the optimal decisions.

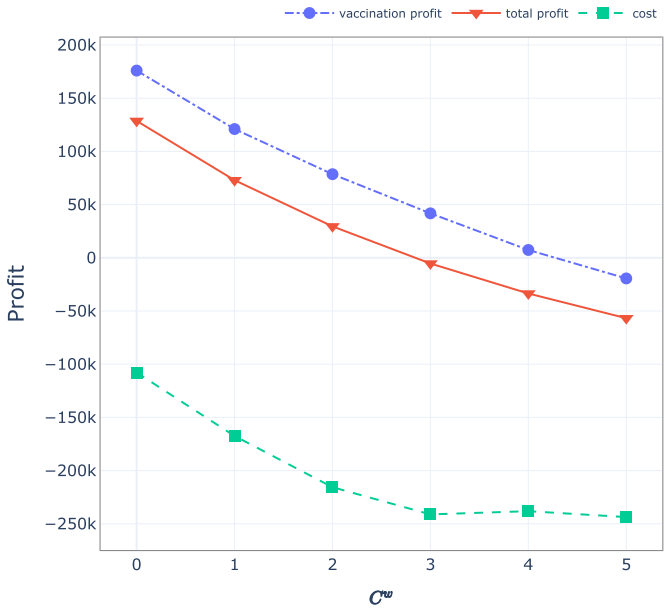

Fig. 7. Impact of the wastage penalty C^w on the profits.

Fig. 9. Impact of the facility fixed cost C^f on the profits.

cost drops in general, there is a little rise from $C^w = 3$ to 4. The reason is that the reduction of the inventory cost sometimes overweighs the increase of the investment cost. Consequently, the solution is quite sensitive to the wastage penalty C^w. With larger values of C^w, the decision-makers tend to take full advantage of the possible vaccine supply and should schedule more vaccinations.

5.4.3. Impact of the facility fixed cost C^f

Figure 8 illustrates the decrease of the three components of the optimal decisions as the facility fixed cost coefficient C^f changes from 3000 to 24,000. The number of opened facilities drops sharply from 15 to 6, and drones from 12 to 7. The scheduled vaccinations show a mild change for about 4000 vials, compared to 80,000 vials by varying C^w in Fig. 6. Moreover, the downward trends of the three profits are observed in Fig. 9. The perturbation in the cost with $C^f = 12,000$ could also be explained by the influence of the inventory cost. Also note that the cost is greatly affected by coefficient C^f, while the total or vaccination profits are less affected under the setting with $\alpha = 5$.

Table 5
Trade-off between profit and vaccination equity.

ξ	Profit			Vaccination rate (%)		
	total	vaccination	cost	θ_{max}	θ_{min}	Gap
0.05	29,265	78,621	217,512	16.1	15.3	5.0
0.1	29,541	78,574	215,623	16.4	14.8	9.7
0.2	30,247	78,625	211,640	17.2	13.8	19.8
0.5	32,728	78,608	196,673	20.6	10.3	50.0
1	40,884	73,381	121,600	100	0	100.0

5.5. Analysis of equity

Vaccine distribution equity is one of the main considerations in our study. Thus, in this section, we analyze the trade-off between equity and profit by changing ξ from 0.05 to 1. The smaller the ξ, the fairer the distribution. Then we compare the facility location and allocation decisions between equitable ($\xi = 0.1$) and inequitable ($\xi = 1$) models.

Table 5 reports the results of profit values and the maximum, the minimum, and their relative gap of vaccination rates under dif-

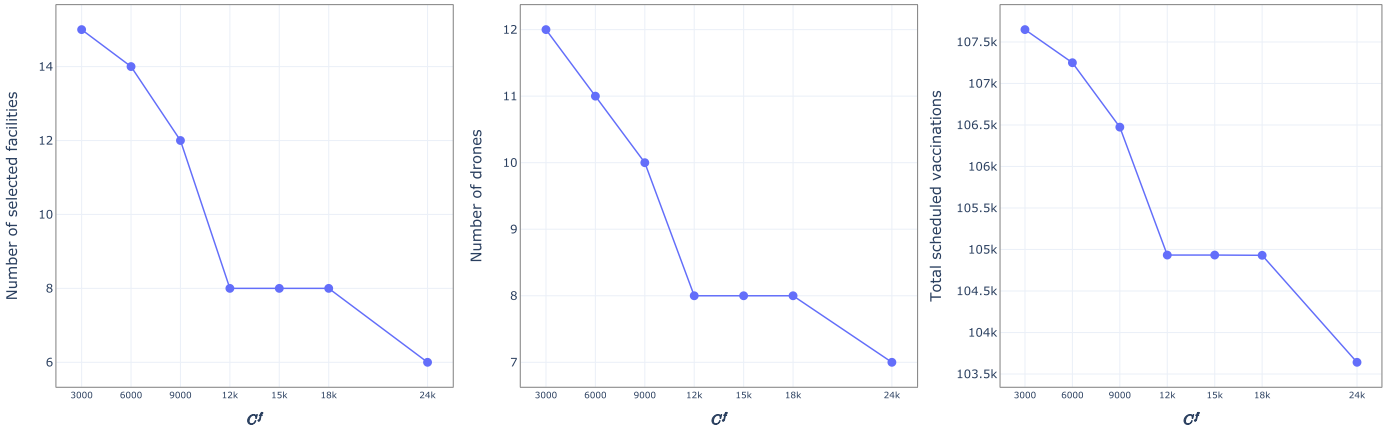

(a) Number of selected facilities (b) Number of drones (c) Total scheduled vaccinations

Fig. 8. Impact of the facility fixed cost C^f on the optimal decisions.

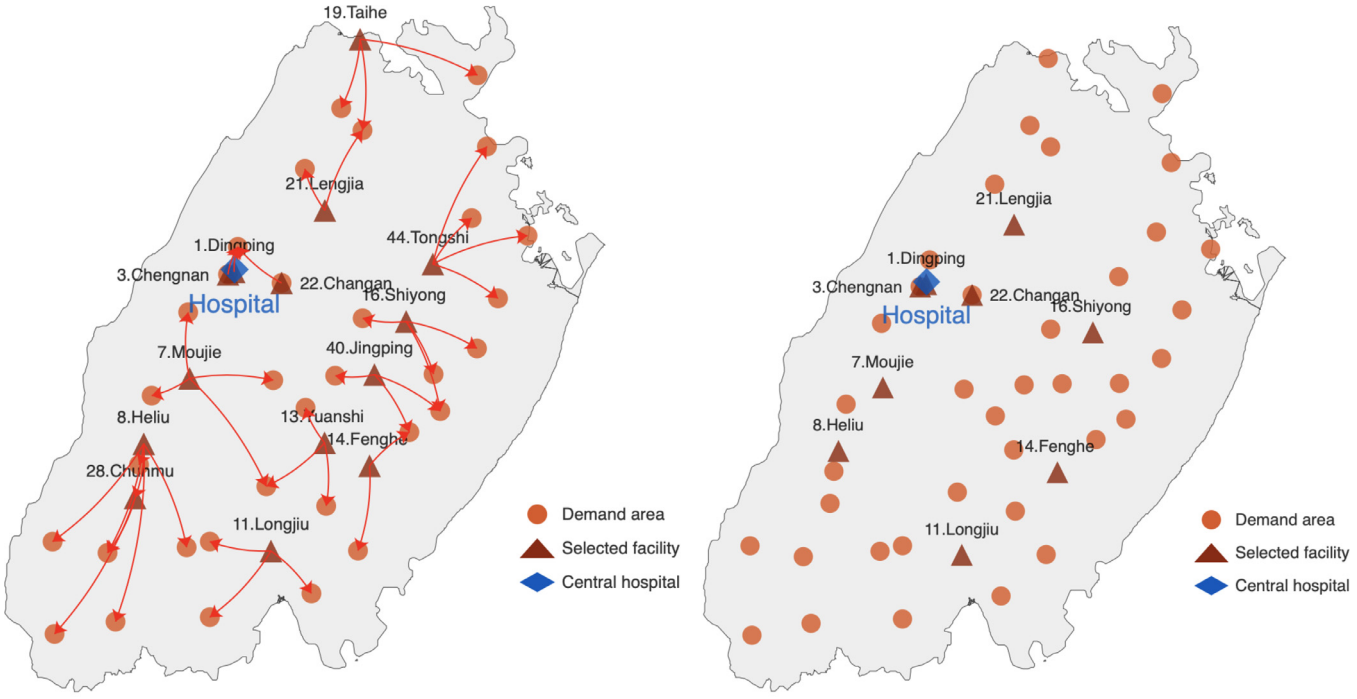

(a) Decisions considering equity ($\xi = 0.1$) (b) Decisions neglecting equity ($\xi = 1$)

Fig. 10. Map of Linshui County with the facility location-allocation decisions considering or neglecting equity.

ferent ξ. With the rise of ξ, which indicates the release of the equity requirement, the total profit goes up and the cost goes down. In contrast, the relative gap between $\theta_{\max}$ and $\theta_{\min}$ in the final result steadily increases, reaching 100% for the problem that completely neglects equity. When the supply of COVID-19 vaccines is limited, they are first distributed to the nearest demand sites to promote the total cost without equity consideration. In a word, equity and profit are a trade-off; equitable vaccine distribution is achieved at the price of higher cost during the vaccine shortage.

To further investigate the insights regarding the facility location-allocation decisions, we display the results of the problems considering ($\xi = 0.1$) and neglecting ($\xi = 1$) equity in Fig. 10. The arc in the figure indicates at least one vaccination assignment throughout the time horizon. No arc can be found in Fig. 10(b) for the decisions neglecting equity, and all vaccines are concentrated at the opened facilities (marked as triangles) to pursue less accessing cost. On the contrary, additional facilities are opened in remote areas like 19.Taihe in the top and 28.Chunmu in the bottom, and all villages are covered under equitable distribution. Actually, without considering equity, facilities near the central hospital with large capability are of higher priority to be selected. To support this conclusion, we list the detailed information of the opened facilities in Table 6. It shows that all facilities with a capability over 7000 are selected, as well as those with 3000 and the least distances (21 Lengjia, 22 Changan). In conclusion, it is particularly essential to address equity when distributing limited vaccine resources; otherwise, vaccines are concentrated into the center or dense areas.

Table 6
Imformation about the opened facilities.

Code	Village	Capability	Distance (km)	Opened facilities	
				Considering equity	Neglecting equity
1	Dingping	10,000	0.2	✓	✓
3	Chengnan	7000	0.8	✓	✓
7	Moujie	7000	10.2	✓	✓
8	Heliu	7000	17.2	✓	✓
11	Longjiu	7000	24	✓	✓
13	Yuanshi	3000	17	✓	
14	Fenghe	7000	21.1	✓	✓
16	Shiyong	7000	17.2	✓	✓
19	Taihe	3000	22.9	✓	
21	Lengjia	3000	10.1	✓	✓
22	Changan	3000	4.7	✓	✓
28	Chunmu	3000	21.6	✓	
33	Longqiao	3000	18.5		
40	Jingping	3000	16.2	✓	
44	Tongshi	3000	19.2	✓	

6. Conclusion and future work

This paper aims to optimize an equitable vaccine distribution problem considering both social and economic benefits. We for the first time, explore a joint vaccination facility location, transportation capacity design, and vaccination scheduling optimization problem, which is tailored to addressing vaccination difficulties in rural areas using drone delivery technologies. This study also fills the research gap where there is little attention on vaccine distribution with supply uncertainty. A two-stage robust model with a budgeted uncertainty set is adopted to tackle this uncertainty. Two tailored column-and-constraint generation algorithms are proposed, where the subproblems are solved via the vertex traversal and the dual methods, respectively. In particular, an MILP reformulation is provided for the nonlinear dual subproblem. We also demonstrate the efficiency of the dual method over the vertex traversal with randomly generated instances.

Real-world data of Linshui County is used to analyze the problem. The results indicate that the robust model outperforms the deterministic model, especially at a large uncertain level. It is really beneficial for decision-makers to account for future supply variation when determining the vaccine distribution plan. Besides, if the

decision-makers are more concerned about the vaccination profit, they are suggested to invest more facilities and drones, and schedule fewer vaccinations to cope with the increased uncertainty. It also notes that the weight coefficient α has a significant impact on balancing the importance of social and economic benefits. The number of scheduled inoculations does not increase with α but efficiently rises with the penalty of vaccine wastage. Another conclusion is that it is particularly necessary to address equity when distributing limited vaccine resources. Otherwise, vaccines are concentrated into the center or dense areas. The results can help the decision-makers to determine a robust and equitable vaccine distribution plan under supply uncertainty when facing vaccine shortages.

For future research, the problem can be extended in the following ways. First of all, the delivery of vaccines to rural areas is only realized by drones in the current network. A hybrid delivery method could be applied, which allows traditional transportation to reach some less vulnerable sites, promoting the efficiency of the distribution. Moreover, the single type (one dose) of vaccine vial could be extended to multiple types in future studies. The use of multi-dose vials can effectively reduce vaccination costs, but comes with a higher risk of open vial wastage. Lastly, our two-stage robust model assumes that the information of uncertain supply of all time periods is realized at once before the second-stage decisions. A multi-stage or dynamic model considering the sequential relationship of decisions over the time periods is suggested for future research.

Declaration of Competing Interest

The authors declare that we have no known competing financial interests or personal relationships that could have appeared to influence the work reported in this paper.

CRediT authorship contribution statement

Xin Wang: Conceptualization, Formal analysis, Investigation, Methodology, Software, Writing – original draft, Writing – review & editing. **Ruiwei Jiang:** Conceptualization, Methodology. **Mingyao Qi:** Conceptualization, Writing – review & editing.

Data availability

No data was used for the research described in the article.

Acknowledgement

This work was supported by the National Natural Science Foundation of China under grant No. 71772100.

Appendix A. Data of Linshui County

Table 7
Data of Linshui County.

Code	Village	Population	Capability	Code	Village	Population	Capability
0	Central hospital	–	–	23	Xitian	7164	–
1	Dingping	113,699	10,000	24	Liangban	9595	–
2	Chengbei	34,671	–	25	Ganba	6668	–
3	Chengnan	31,079	7000	26	Sihai	8611	–
4	Ganzi	13,268	–	27	Qiufeng	4033	–
5	Longan	10,943	–	28	Chunmu	6750	3000
6	Guanyinqiao	17,351	–	29	Huaying	2501	–
7	Moujie	14,851	7000	30	Zizhong	9051	–
8	Heliu	13,958	7000	31	Fengya	5479	–
9	Tantong	28,559	–	32	Lijia	8314	–
10	Gaotan	20,691	–	33	Longqiao	11,015	3000
11	Longjiu	44,582	7000	34	Guanhe	7700	–
12	Yulin	18,886	–	35	Lianghe	7057	–
13	Yuanshi	19,040	3000	36	Changtan	9690	–
14	Fenghe	37,632	7000	37	Liangshan	6950	–
15	Baer	10,639	–	38	Fusheng	13,460	–
16	Shiyong	20,779	7000	39	Gulu	5586	–
17	Xingren	17,736	–	40	Jingping	8316	3000
18	Wangjia	16,760	–	41	Liutang	8921	–
19	Taihe	12,457	3000	42	Shizi	12,195	–
20	Xinzhen	5353	–	43	Hulin	8753	–
21	Lengjia	7001	3000	44	Tongshi	3626	3000
22	Changan	11,746	3000	45	Sangu	11,579	–

References

[1] Acharya KP, Ghimire TR, Subramanya SH. Access to and equitable distribution of COVID-19 vaccine in low-income countries. npj Vaccines 2021;6(1):1–3.
[2] An Y, Zeng B, Zhang Y, Zhao L. Reliable *p*-median facility location problem: two-stage robust models and algorithms. Transp Res Part B 2014;64:54–72.
[3] Ardestani-Jaafari A, Delage E. The value of flexibility in robust location–transportation problems. Transp Sci 2018;52(1):189–209.
[4] Atamtürk A, Zhang M. Two-stage robust network flow and design under demand uncertainty. Oper Res 2007;55(4):662–73.
[5] Azadi Z., Eksioglu S.D., Geismar H.N.. Optimization of distribution network configuration for pediatric vaccines using chance constraint programming. arXiv preprint arXiv:2006.05488
[6] Azadi Z, Gangammanavar H, Eksioglu S. Developing childhood vaccine administration and inventory replenishment policies that minimize open vial wastage. Ann Oper Res 2020;292(1):215–47.
[7] Balcik B, Yucesoy E, Akca B, Karakaya S, Gevsek AA, Baharmand H, et al. A mathematical model for equitable in-country COVID-19 vaccine allocation. Int J Prod Res 2022;60(24):7502–26.
[8] Bandi C., Gao S.Y., Moorthy R., Teo C.-P., Toh K.-C.. Vaccine appointment scheduling: the second dose challenge. Available at SSRN 39097922021.
[9] Ben-Tal A, El Ghaoui L, Nemirovski A. Robust optimization. Princeton University Press; 2009. chap. Preface
[10] Bertsimas D, Sim M. The price of robustness. Oper Res 2004;52(1):35–53.
[11] Chen SI, Norman BA, Rajgopal J, Assi TM, Lee BY, Brown ST. A planning model for the WHO-EPI vaccine distribution network in developing countries. IIE Trans 2014;46(8):853–65.
[12] Chen S-I, Norman BA, Rajgopal J, Lee BY. Passive cold devices for vaccine supply chains. Ann Oper Res 2015;230(1):87–104.
[13] Chen X., Li M., Simchi-Levi D., Zhao T.. Allocation of COVID-19 vaccines under limited supply. Available at SSRN 36789862020;.
[14] Cheng C, Adulyasak Y, Rousseau L-M. Robust facility location under demand uncertainty and facility disruptions. Omega 2021;103:102429.
[15] Chung SH, Sah B, Lee J. Optimization for drone and drone-truck combined operations: a review of the state of the art and future directions. Comput Oper Res 2020:105004.
[16] Conforti M, Cornuéjols G, Zambelli G, et al. Integer programming, vol 271. Springer; 2014.
[17] Cooper L. The transportation-location problem. Oper Res 1972;20(1):94–108.
[18] Crainic TG, Laporte G. Planning models for freight transportation. Eur J Oper Res 1997;97(3):409–38.
[19] De Boeck K, Decouttere C, Vandaele N. Vaccine distribution chains in low-and middle-income countries: a literature review. Omega 2019:97:102097.
[20] Delage E. Quantitative risk management using robust optimization. Lecture notes. HEC Montréal; 2017. chapter Exact solution methods for robust two-stage problems
[21] Duijzer LE, Van Jaarsveld W, Dekker R. Literature review: the vaccine supply chain. Eur J Oper Res 2018;268(1):174–92.
[22] Enayati S, Özaltın OY. Optimal influenza vaccine distribution with equity. Eur J Oper Res 2020;283(2):714–25.
[23] Fadaki M, Abareshi A, Far SM, Lee PT-W. Multi-period vaccine allocation model in a pandemic: a case study of COVID-19 in australia. Transp Res Part E 2022;161:102689.
[24] Gabrel V, Lacroix M, Murat C, Remli N. Robust location transportation problems under uncertain demands. Discrete Appl Math 2014;164:100–11.
[25] Georgiadis GP, Georgiadis MC. Optimal planning of the COVID-19 vaccine supply chain. Vaccine 2021;39(37):5302–12.
[26] Gilani H, Sahebi H. A data-driven robust optimization model by cutting hyperplanes on vaccine access uncertainty in COVID-19 vaccine supply chain. Omega 2022;110:102637.
[27] Habibi F, Abbasi A, Chakrabortty RK. Designing an efficient vaccine supply chain network using a two-phase optimization approach: a case study of COVID-19 vaccine. Int J Syst Sci 2022;10(1):2121623.
[28] Haidari LA, Brown ST, Ferguson M, Bancroft E, Spiker M, Wilcox A, Ambikapathi R, Sampath V, Connor DL, Lee BY. The economic and operational value of using drones to transport vaccines. Vaccine 2016;34(34):4062–7.
[29] Horst R, Tuy H. Global optimization: deterministic approaches. Springer Science & Business Media; 2013.
[30] IRC. The only way to stop COVID-19? Vaccines for all. International Rescue Committee; 2021. https://www.rescue.org/article/only-way-stop-covid-19-vaccines-all.
[31] Jahani H, Chaleshtori AE, Khaksar SMS, Aghaie A, Sheu J-B. COVID-19 vaccine distribution planning using a congested queuing system-a real case from australia. Transp Res Part E 2022;163:102749.
[32] Jarumaneeroj P, Dusadeerungsikul PO, Chotivanich T, Nopsopon T, Pongpirul K. An epidemiology-based model for the operational allocation of COVID-19 vaccines: a case study of thailand. Comput Ind Eng 2022;167:108031.
[33] Krumke SO, Schmidt E, Streicher M. Robust multicovers with budgeted uncertainty. Eur J Oper Res 2019;274(3):845–57.
[34] Kumar A., Kumar G., Ramane T.V., Singh G. Optimal COVID-19 vaccine stations location and allocation strategies. Benchmarking: an international journal 2022;(ahead-of-print) https://doi.org/10.1108/BIJ-02-2022-0089.
[35] Lai X, Lu X, Yu X, Zhu N. Multi-period integrated planning for vaccination station location and medical professional assignment under uncertainty. Comput Ind Eng 2021;161:107673.
[36] Lee BY, Assi T-M, Rookkapan K, Wateska AR, Rajgopal J, Sornsrivichai V, Chen S-I, Brown ST, Welling J, Norman BA, et al. Maintaining vaccine delivery following the introduction of the rotavirus and pneumococcal vaccines in thailand. PLoS One 2011;6(9):e24673.
[37] Lee BY, Brown ST, Bailey RR, Zimmerman RK, Potter MA, Mcglone SM, Cooley PC, Grefenstette JJ, Zimmer SM, Wheaton WD. The benefits to all of ensuring equal and timely access to influenza vaccines in poor communities. Health Aff 2011;30(6):1141–50.
[38] Lee BY, Wedlock PT, Haidari LA, Elder K, Potet J, Manring R, Connor DL, Spiker ML, Bonner K, Rangarajan A, et al. Economic impact of thermostable vaccines. Vaccine 2017;35(23):3135–42.
[39] Li X, Pan Y, Jiang S, Huang Q, Chen Z, Zhang M, Zhang Z. Locate vaccination stations considering travel distance, operational cost, and work schedule. Omega 2021;101:102236.
[40] Lim J, Claypool E, Norman BA, Rajgopal J. Coverage models to determine outreach vaccination center locations in low and middle income countries. Oper Res Health Care 2016;9:40–8.
[41] Lin Q, Zhao Q, Lev B. Influenza vaccine supply chain coordination under uncertain supply and demand. Eur J Oper Res 2021;297(3):930-948.
[42] Lopes JM, Morales CC, Alvarado M, Melo VAZC, Paiva LB, Dias EM, Pardalos PM. Optimization methods for large-scale vaccine supply chains: a rapid review. Ann Oper Res 2022;316(1):699–721.
[43] Macrina G, Pugliese LDP, Guerriero F, Laporte G. Drone-aided routing: a literature review. Transp Res Part C 2020;120:102762.
[44] Marandi A, van Houtum G-J. Robust location-transportation problems with integer-valued demand. Optim Online 2020. http://www.optimization-online.org/DB_HTML/2020/01/7559.html.
[45] Marsh MT, Schilling DA. Equity measurement in facility location analysis: areview and framework. Eur J Oper Res 1994;74(1):1–17.
[46] Mofrad MH, Maillart LM, Norman BA, Rajgopal J. Dynamically optimizing the administration of vaccines from multi-dose vials. IIE Trans 2014;46(7):623–35.
[47] Mohammadi M, Dehghan M, Pirayesh A, Dolgui A. Bi-objective optimization of a stochastic resilient vaccine distribution network in the context of the COVID-19 pandemic. Omega 2022;113:102725.
[48] Otto A, Agatz N, Campbell J, Golden B, Pesch E. Optimization approaches for civil applications of unmanned aerial vehicles (UAVs) or aerial drones: a survey. Networks 2018;72(4):411–58.
[49] Pazirandeh A. Sourcing in global health supply chains for developing countries: literature review and a decision making framework. Int J Phys Distrib Logist Manag 2011;41(4):364-384.
[50] Rahman HF, Chakrabortty RK, Paul SK, Elsawah S. Optimising vaccines supply chains to mitigate the COVID-19 pandemic. Int J Syst Sci 2022;10(1):212275.
[51] Rastegar M, Tavana M, Meraj A, Mina H. An inventory-location optimization model for equitable influenza vaccine distribution in developing countries during the COVID-19 pandemic. Vaccine 2021;39(3):495–504.
[52] Roos E, den Hertog D. Reducing conservatism in robust optimization. INFORMS J Comput 2020;32(4):1109–27.
[53] Tang L, Li Y, Bai D, Liu T, Coelho LC. Bi-objective optimization for a multi-period COVID-19 vaccination planning problem. Omega 2022;110:102617.
[54] Tavana M., Govindan K., Nasr A.K., Heidary M.S., Mina H. A mathematical programming approach for equitable COVID-19 vaccine distribution in developing countries. Ann Oper Res 2021; doi:10.1007/s10479-021-04130-z.
[55] Terry M.. Updated comparing COVID-19 vaccines: timelines, types and prices. BioSpace2021; https://www.biospace.com/article/comparing-covid-19-vaccines-pfizer-biontech-moderna-astrazeneca-oxford-j-and-j-russia-s-sputnik-v/.
[56] UN. Covid vaccines: widening inequality and millions vulnerable. UN News2021;https://news.un.org/en/story/2021/09/1100192.
[57] Vincent J. Self-flying drones are helping speed deliveries of COVID-19 vaccines in Ghana. Theverge; 2021. https://www.theverge.com/2021/3/9/22320965/drone-delivery-vaccine-ghana-zipline-cold-chain-storage
[58] WHO. Module 2: the vaccine cold chain. Immunization in practice: a practical guide for health staff. World Health Organization; 2015.
[59] WHO. COVID-19 vaccine tracker and landscape. World Health Organization; 2020. https://www.who.int/publications/m/item/draft-landscape-of-covid-19-candidate-vaccines
[60] WHO, UNDP, Oxford University, Global dashboard for vaccine equity. Data Futures Platform2021;https://data.undp.org/vaccine-equity/.
[61] Yang Y, Rajgopal J. Outreach strategies for vaccine distribution: a multi-period stochastic modeling approach. Oper Res Forum 2021;2(2): 24.
[62] Yarmand H, Ivy JS, Denton B, Lloyd AL. Optimal two-phase vaccine allocation to geographically different regions under uncertainty. Eur J Oper Res 2014;233(1):208–19.
[63] Yi M, Marathe A. Fairness versus efficiency of vaccine allocation strategies. Value Health 2015;18(2):278–83.
[64] Zeng B, Zhao L. Solving two-stage robust optimization problems using a column-and-constraint generation method. Oper Res Lett 2013;41(5):457–61.
[65] Zhang C, Li Y, Cao J, Wen X. On the mass COVID-19 vaccination scheduling problem. Comput Oper Res 2022;141:105704.